AD-A042 906 CIVIL ENGINEERING LAB (NAVY) PORT HUENEME CALIF F/G 13/13
DYNAMIC LOADING EFFECTS ON EMBEDMENT ANCHOR HOLDING CAPACITY.(U)
JUL 77 Z M GOUDA, D G TRUE

UNCLASSIFIED CEL-TN-1489 NL

1 OF 1
ADA042906

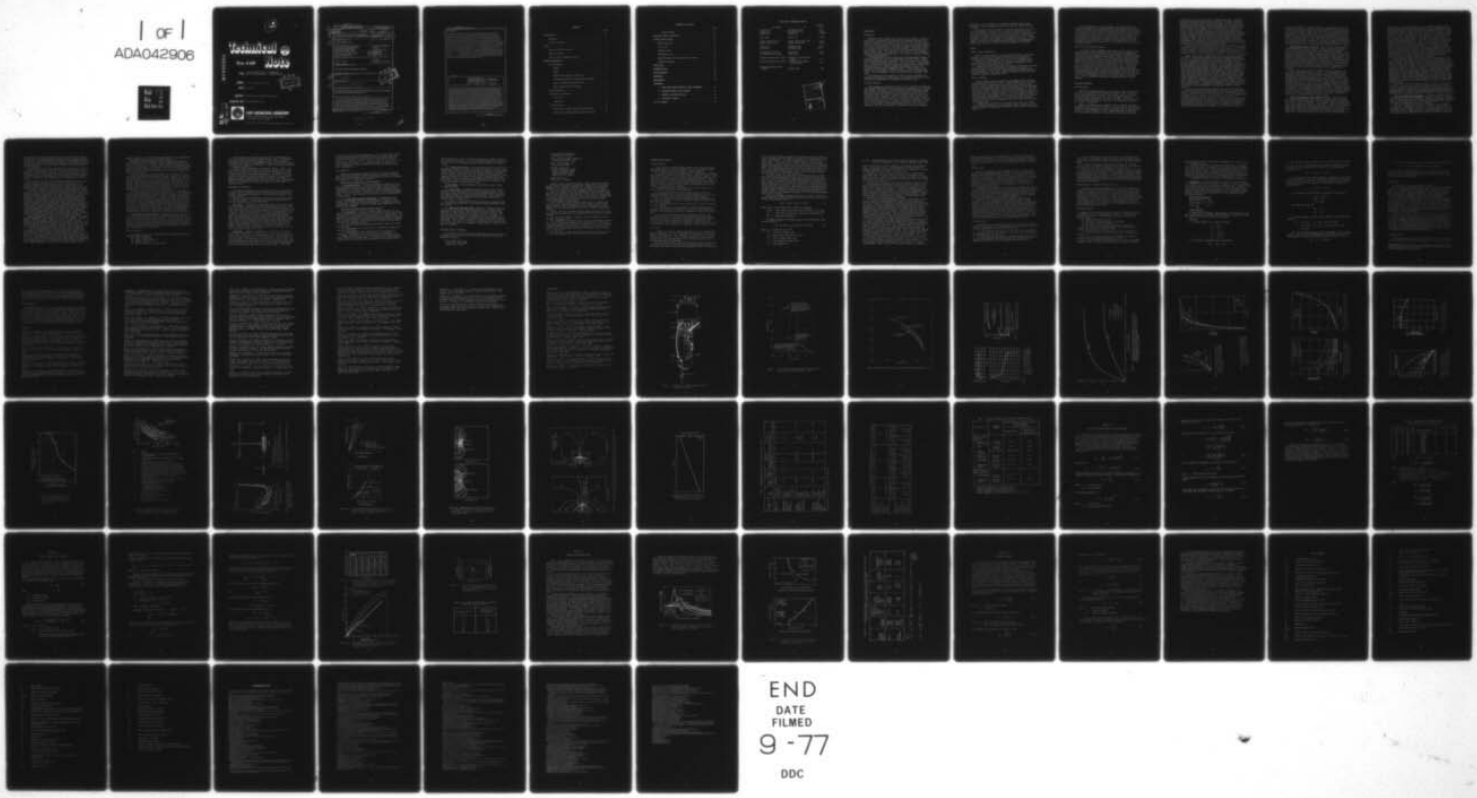

END
DATE FILMED
9-77
DDC

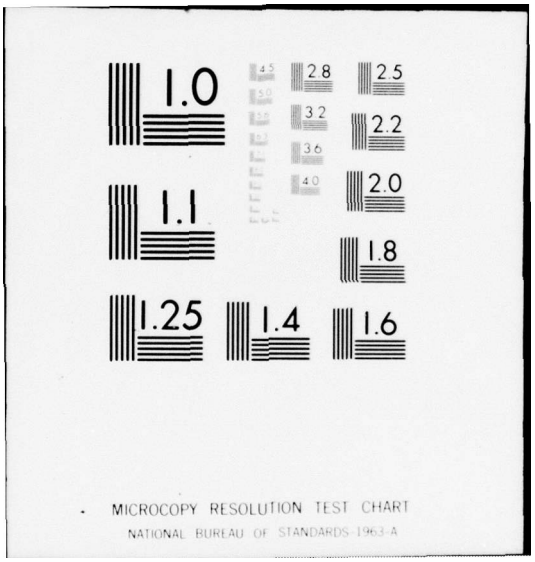
1.0
1.1
1.25
1.4
1.6
1.8
2.0
2.2
2.5
2.8
3.2
3.6
4.0
4.5
5.0
MICROCOPY RESOLUTION TEST CHART
NATIONAL BUREAU OF STANDARDS-1963-A

Technical Note

CEL

TN no. N-1489

title: DYNAMIC LOADING EFFECTS ON EMBEDMENT ANCHOR HOLDING CAPACITY — INTERIM REPORT

author: Z. M. Gouda and D. G. True

date: July 1977

sponsor: Naval Facilities Engineering Command

program nos: YF52.556.091.01.104

CIVIL ENGINEERING LABORATORY
NAVAL CONSTRUCTION BATTALION CENTER
Port Hueneme, California 93043

Unclassified

SECURITY CLASSIFICATION OF THIS PAGE (When Data Entered)

REPORT DOCUMENTATION PAGE		READ INSTRUCTIONS BEFORE COMPLETING FORM
1. REPORT NUMBER CEL-TN-1489	2. GOVT ACCESSION NO. DN587007	3. RECIPIENT'S CATALOG NUMBER Rept.
4. TITLE (and Subtitle) DYNAMIC LOADING EFFECTS ON EMBEDMENT ANCHOR HOLDING CAPACITY - INTERIM REPORT		5. TYPE OF REPORT & PERIOD COVERED Interim Jul 1974 - Dec 1975 6. PERFORMING ORG. REPORT NUMBER
7. AUTHOR(s) Z. M. Gouda and D. G. True		8. CONTRACT OR GRANT NUMBER(s)
9. PERFORMING ORGANIZATION NAME AND ADDRESS CIVIL ENGINEERING LABORATORY Naval Construction Battalion Center Port Hueneme, California 93043		10. PROGRAM ELEMENT, PROJECT, TASK AREA & WORK UNIT NUMBERS 62759N; YF52.556.091.01.104
11. CONTROLLING OFFICE NAME AND ADDRESS Naval Facilities Engineering Command Alexandria, Virginia 22332		12. REPORT DATE July 1977 13. NUMBER OF PAGES 69
14. MONITORING AGENCY NAME & ADDRESS (if different from Controlling Office) 12 68p.		15. SECURITY CLASS. (of this report) Unclassified 15a. DECLASSIFICATION/DOWNGRADING SCHEDULE

16. DISTRIBUTION STATEMENT (of this Report)

Approved for public release; distribution unlimited.

16 F52556

17. DISTRIBUTION STATEMENT (of the abstract entered in Block 20, if different from Report)

18. SUPPLEMENTARY NOTES

17 YF52556091

19. KEY WORDS (Continue on reverse side if necessary and identify by block number)

Soils, marine soils, dynamics, cyclic loading, earthquake response, anchors, cable strumming, wave loading, current loading, embedment anchors.

20. ABSTRACT (Continue on reverse side if necessary and identify by block number)

This report provides interim guidelines for designers of dynamically loaded seafloor foundations and anchors based on available knowledge of terrestrial and seafloor soils. Investigations of the response of selected seafloor soils to dynamically induced forces are reported, and the development of standardized design procedures for propellant-actuated direct embedment anchors is presented. These procedures must account for the strength of seafloor soils over the short and the long term around a seafloor embedment anchor

continued

DD FORM 1 JAN 73 1473 EDITION OF 1 NOV 65 IS OBSOLETE

Unclassified

SECURITY CLASSIFICATION OF THIS PAGE (When Data Entered)

391 111

20. Continued

sustaining static and dynamic loads. Important findings were that the soil parameters relevant to the holding capacity of deeply embedded propellant-actuated anchors are: soil moduli, creep, suction, cyclic strength loss, stress-strain relationships under dynamic loading, and responses to shock and slow loading. Some anchor-related parameters are: (a) the anchor embedment depth, buoyant weight, angle-of-line pull, and size and shape of flukes; and (b) magnitudes of the static and dynamic components of loading and the dynamic loading period for loads produced in the line by current fluctuations, waves, vortex shedding, impact, or line snap, and for loads produced more or less simultaneously in the line and the sediment by earthquakes or underwater blasts. It is recommended that planners use the interim design guidelines in this report for the engineering of embedment anchors to sustain dynamic loading until revised guidelines are developed. Field data from dynamically loaded embedment anchor moorings in actual use and other operating seafloor structures should be collected over extended periods of time for use in verifying and refining the present design methods. Revised guidelines should be available in 1978.

Library Card

Civil Engineering Laboratory
DYNAMIC LOADING EFFECTS ON EMBEDMENT ANCHOR HOLDING CAPACITY – INTERIM REPORT, by Z. M. Gouda and D. G. True
TN-1489 69 pp illus July 1977 Unclassified

1. Seafloor anchors and foundations 2. Dynamic loading I. YF52.556.091.01.104

This report provides interim guidelines for designers of dynamically loaded seafloor foundations and anchors based on available knowledge of terrestrial and seafloor soils. Investigations of the response of selected seafloor soils to dynamically induced forces are reported, and the development of standardized design procedures for propellant-actuated direct embedment anchors is presented. These procedures must account for the strength of seafloor soils over the short and the long term around a seafloor embedment anchor sustaining static and dynamic loads. Important findings were that the soil parameters relevant to the holding capacity of deeply embedded propellant-actuated anchors are: soil moduli, creep, suction, cyclic strength loss, stress-strain relationships under dynamic loading, and responses to shock and slow loading. Some anchor-related parameters are: (a) the anchor embedment depth, buoyant weight, angle-of-line pull, and size and shape of flukes; and (b) magnitudes of the static and dynamic components of loading and the dynamic loading period for loads produced in the line by current fluctuations, waves, vortex shedding, impact, or line snap, and for loads produced more or less simultaneously in the line and the sediment by earthquakes or underwater blasts. It is recommended that planners use the interim design guidelines in this report for the engineering of embedment anchors to sustain dynamic loading until revised guidelines are developed. Field data from dynamically loaded embedment anchor moorings in actual use and other operating seafloor structures should be collected over extended periods of time for use in verifying and refining the present design methods. Revised guidelines should be available in 1978.

CONTENTS

	Page
INTRODUCTION	1
Background	1
Technical Approach	1
SCOPE	2
Types of Soils Encountered	2
Types of Loading	2
Types of Direct Embedment Anchors	3
RELEVANT PARAMETERS	3
Soil Parameters	3
Moduli	3
Creep	4
Negative Pore Pressure (Suction)	5
Stress-Strain Behavior Under Dynamic Loading	5
Loss of Strength and Liquefaction	6
Shock Loading and Slow Loading	8
Anchor Parameters	8
Environmental Parameters	9
Pore Fluid	9
Temperature	9
Load Parameters	10
Rapid Cyclic Loading (With Inertial Forces)	10
Slow Cyclic Loading (Without Inertial Forces)	10

CONTENTS (Continued)

	Page
Shock Loading.	11
AVAILABLE TESTING TECHNIQUES	11
INTERIM DESIGN METHODS	13
General Approach.	13
Line Loads	13
Sediment Loads	16
Earthquake Loads	16
Design Features for Reducing Dynamic Effects	16
Analytical Example.	16
CONCLUSIONS.	20
RECOMMENDATIONS.	20
FUTURE RESEARCH.	21
REFERENCES	21
BIBLIOGRAPHY	26
APPENDIXES	
A - LOADS FROM VORTEX SHEDDING (CABLE STRUMMING).	45
B - RADIATION DAMPING AND STIFFNESS	49
C - DYNAMIC LOAD MAGNIFICATION.	54
D - HYSTERETIC DAMPING.	58
LIST OF SYMBOLS.	61

ENGLISH-SI CONVERSION FACTORS

To convert	To	Multiply by
inches (in.)	millimeters (mm)	25.40
inches (in.)	centimeters (cm)	2.540
inches (in.)	meters (m)	0.0254
feet (ft)	meters (m)	0.305
square inches (sq in.)	square centimeters (cm^2)	6.45
square feet (sq ft)	square meters (m^2)	0.093
pounds (lb)	kilograms (kg)	0.453
tons (ton)	kilograms (kg)	907.2
one pound force (lbf)	newtons (N)	4.45
one kilogram force (kgf)	newtons (N)	9.81
pounds per square foot (psf)	newtons per square meter (N/m^2)	47.9
pounds per square inch (psi)	kilonewtons per square meter (kN/m^2)	6.9
newtons per square meter (N/m^2)	pascals (Pa)	1.00

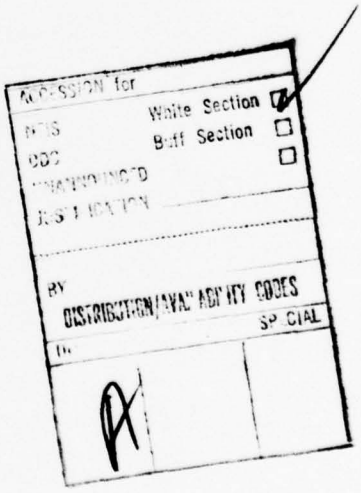

INTRODUCTION

Background

Embedment anchor systems used to moor surface vessels or buoys are subjected to a combination of sustained and repeated loads that vary with the tautness of the system and the nature of wave or tidal action. Studies on terrestrial soils have indicated that soil-structure systems do not react in the same way to sustained, repeated loadings as they do to strictly sustained loads of the same magnitude. Most dynamic tests on terrestrial soils show a decrease in soil strength values as well as lower failure levels. For this reason the design of direct embedment anchors should include consideration of the effects of dynamic loadings on anchor holding capacity.

A program sponsored by the Naval Facilities Engineering Command, is presently underway at the Civil Engineering Laboratory (CEL) to determine the dynamic response of seafloor soils as it affects the performance of Navy anchors and foundations. Other objectives of this program are to determine the response of selected seafloor soils to dynamically induced forces and to develop standardized design procedures for propellant-actuated direct embedment anchors. These procedures must account for the strengths of seafloor soils over short and long terms around a deep sea embedment anchor sustaining static and dynamic loadings.

This report has been prepared to provide interim guidelines for designers of dynamically loaded seafloor foundations and anchors, based upon available knowledge of terrestrial and seafloor soils.

Technical Approach

The response of terrestrial soils to cyclic and static loadings has been studied extensively, both experimentally and analytically. However, deep seafloor soils tend to be more normally consolidated than terrestrial soils, more homogeneous, and more frequently composed of fragile particles such as the calcareous or silicious skeletons of small- to microscopic-sized organisms. Seafloor soils have been studied mostly statically; only a limited amount of investigation has been carried out on their behavior under cyclic loading. Because the strength of terrestrial soils has been found to decrease considerably under cyclic loadings, it is necessary to determine dynamic seafloor soil properties insofar as they may affect seafloor foundation and anchor performance.

Specifically, it is necessary to accurately identify critical soil conditions, loss of strength, and failure around the loaded foundation or anchor.

The present technical approach to this problem consists of predicting the response of seafloor soils to dynamic loading by using the available technical knowledge of the static versus the dynamic properties of terrestrial soils in conjunction with measured static engineering properties of seafloor soils, and by also measuring the cyclic loading response of seafloor soil samples if the expense is warranted. In this report, the details of this approach are described, and improvements expected to be made as a result of current research are discussed.

SCOPE

Types of Soils Encountered

Data for typical seafloor soils are given in Table 1, including sampling locations, water depths, Atterberg limits, average soil strengths at the sampled depths (0 to 35 ft), and soil sensitivity.

Evaluation of the behavior and performance of embedment anchors under repeated loadings requires the accurate determination of the static and dynamic properties of such soils.

Presently, little is known about the possible differences in dynamic behavior between terrestrial soils and such seafloor soils as the calcareous oozes -- that contain large fractions of crushable grains -- and the turbidites -- that have a relatively metastable structure when compared to granular terrestrial soils.

Types of Loading

Dynamic anchor loads are applied to the embedded anchor through either the soil or the anchor line. Dynamic loading can also be transmitted through the anchor line; such a load can be caused by line motion from drag changes under current fluctuations or by the phenomenon of cable strumming (oscillatory line motions perpendicular to the line axis and the current direction) forced by vortex shedding in a more-or-less steady current. Dynamic line load also can be caused by impact of the moored object with another object, or by line snapping caused by the heave and surge displacements of the moored object under the influence of surface waves and wind forces. On a short-term basis, however, dynamic loads can result from seismic motions and blast-induced subseafloor shock waves.

Dynamic loads can produce a load magnification when the loading rate or frequency happens to coincide with a natural frequency of the moored system or its components (oscillated object, anchor, and seafloor soil).

On the application of dynamic loading, the stress distribution around the embedded anchor is changed due to the increase or decrease of "locked in" pressures, previously developed under normal static loads. In the extreme, dynamic loading can cause the reduction of soil strength, to a large degree in the case of cohesive soils, and to the extent of liquefaction for granular soils. On the removal of the dynamic load, soil properties and strength characteristics are different than they were under the original static loading. This dynamic loss of soil strength has been studied extensively for terrestrial soils, but not yet for seafloor soils.

Types of Direct Embedment Anchors

The types of direct embedment anchors that are of concern in this report are those which are embedded on a direct path (as opposed to being augered in, for example) after being launched or dropped downward to attain the energy required for embedment. Several such anchors have been and are being developed by CEL, including the CEL 20K propellant anchor shown in Figure 1 (Taylor, 1976), the CEL 10K propellant anchor (Wadsworth, 1976), and the CEL 100K propellant anchor (True and Taylor, 1975). Such anchors consist of two major parts: (1) a launcher and (2) a projectile, which includes a piston and a fluke. Fluke sizes differ in dimensions and shape for use in various types of seafloor sediments as well as rocks. Sediment flukes are plate-like projectiles with attachments that cause keying after embedment. The rock fluke is a finned, arrowhead-shaped projectile that penetrates the rock and also can key like the sediment fluke for use in dense sand or very stiff clay. Table 2 summarizes the physical dimensions and use of these anchors.

RELEVANT PARAMETERS

Soil Parameters

Basic soil response parameters are required to describe the short-term and long-term mechanical behavior of seafloor soils. From the basic test measurements of stress, strain, phase angle, and frequency, various behavioral characteristics, such as modulus, compliance, viscosity, energy dissipation, and loss of strength, can be calculated. In the following pages the most pertinent soil parameters related to the problem are discussed.

Moduli. An important soil parameter used to describe the dynamic behavior of soils is the shear modulus G. Ground response involving no residual soil displacements is usually determined from the shear modulus of the soil under symmetrical cyclic loading conditions. The shear modulus is usually expressed as the secant modulus determined by the

extreme points on a hysteresis loop on stress-strain axes. The shear modulus depends mainly on the strain amplitude. As strain amplitude increases, the shear (secant) modulus decreases, as shown by the data presented by Thiers (1965) for San Francisco Bay mud. In Figure 2, the measured shear modulus values varied, depending upon the strain amplitude, decreasing from 225KSF at $4.5 \times 10^{-4}\%$ strain to 20 KSF at 1% strain. Also, it is shown in Figure 2 that the shear modulus values for San Francisco Bay mud, determined by Thiers using laboratory testing equipment (dynamic simple shear device), at low strains, are only half of those obtained by in situ wave velocity measurements (Aisiks and Tarshansky, 1968). This decrease may have been caused by increased disturbance in the laboratory tests as compared with the in situ tests. At high strains, measured values are shown to approach values calculated from equations given by Hardin and Drnevich (1972).

Variations in clay characteristics in terms of shear modulus can be expressed by normalizing the shear modulus G with respect to the undrained shear strength S_u and expressing the relationship G/S_u as a function of shear strain. An increase in the cyclic shear strain (Figure 3) causes a reduction in the shear modulus specially at the first few pulses.

Creep. Very little is known about the creep response of seafloor soils. It is anticipated, however, that their creep characteristics will not be any worse than those of the worst terrestrial soils (almost all over-consolidated, organic, stiff fissured clay shale, and low residual strength soils tend to exhibit a high creep rate). Many cohesive sediments are susceptible to shear creep, whereby long-term shear straining occurs under constant loading. The continuing increase of shear creep displacements with time eventually leads to a complete failure of the soil (creep rupture). The magnitude of stress required to cause this creep failure has been found for terrestrial soils to be as low as 60% of the short-term soil strength (Singh and Mitchell, 1968). Creep of embedment anchors can occur if a load less than the ultimate holding capacity of the anchor is applied for an extended period of time. Under these conditions, the anchor eventually might be displaced upward significantly. As the holding capacity of the anchor is lower at a shallower depth of embedment, a relatively constant creep strength would result in an acceleration of the process, leading to anchor pullout.

Creep rate also may increase significantly under cyclic loading. In 1966, Seed and Chan found that seismic loading could trigger increments of creep strain in San Francisco Bay mud. Soil samples were first loaded up to 65% of their static strength for a period of 2 months while recording all strain levels. Creep movements were found to be insignificant except for the first day. Another sample was tested under the same conditions but was dynamically loaded with a simulated earthquake loading at the end of the first day. An immediate increase in axial strain from about 5.5% to about 12% occurred for the first day, and axial strain continued to increase up to 24% through a period of

13 days (see Figure 4). Such a tendency for creep movement after the application of pulsating stresses has been confirmed for the same type of soil and condition by Holzer and Hoeg (1973). The strain versus time curves given in Figure 5 show rapid strain increases immediately after the application of the seismic load; a strain increment of about 4% is shown for a stress level of 70%. These results show that the application of earthquake loads or other vibratory forces to creep-susceptible clay soils can increase creep sharply, and that although the forces may not cause immediate soil failure, the resulting increased creep deformations may be sufficient to lead to failure after some period of time.

Negative Pore Pressure (Suction). When a load is first applied to an anchor embedded in soil, it may be carried by shearing stresses in the soil over and around the anchor or by negative pore pressure (suction) in the water contained by the soil beneath the anchor. With time, any negative pore pressure changes caused by anchor loading will dissipate, resulting in a decrease of the anchor holding capacity. Dissipation of negative pore pressure depends mainly on the ease of water flow in the soil beneath the anchor. If the soil is coarse-grained and pervious, negative pore pressure will dissipate very rapidly, reducing the initially apparent effect of suction considerably. On the other hand if the soil is a fine-grained silt or clay, a considerable amount of time may be required for the dissipation of the negative pore pressures.

Only a very limited amount of research has been conducted to investigate the magnitude of suction forces. The measurements in Duke tests (Ali, 1968) with 3-in.-diam plate anchors on the soil surface indicated an average suction of 2.8 psi. In research carried out by the Hydro-Electric Power Commission of Ontario, laboratory tests were performed with vented and unvented flukes in soft (S_u = 1.5 to 2.5 psi) and stiff (S_u = 14 to 25 psi) clay soils. Figure 6 shows the results of this investigation in the form of a relationship between the uplift coefficient N_u and the relative embedment depth D/B. Such a plot gives an indication of the magnitude of the suction effect on embedded anchors at different relative depths, indicating an increase in N_u, attributable to suction, by a factor approaching about 2.0 at large embedment depths. Hence, the effect of suction forces must be considered in relating short-term to long-term dynamic holding capacity.

Stress-Strain Behavior Under Dynamic Loading. The determination of a dynamic stress-strain relationship for a particular soil, anchor, and loading requires duplication of the boundary conditions existing in the field as closely as possible. Using dynamic triaxial testing equipment, soil stress-strain behavior under cyclic loading can be determined. Under these conditions, the lateral expansion of the soil usually is permitted to exceed the corresponding field amount, and the slope of the stress-strain curve will decrease with the increase of the applied axial load. Some stress-strain curve data have been obtained under the

condition of no lateral expansion of the soil sample (Davisson, 1965; Zaccor and Wallace, 1963). The influence of lateral deformation on soil stress-strain data is illustrated by the stress-strain curves for granular materials shown in Figure 7 for the cases of all-round equal stress (curve A), lateral strain equal to zero (curve B), and constant lateral stress (curve C). Similar behavior is exhibited by cohesive materials in a drained state Bishop (1971). The type of shear test also influences stress-strain behavior. Theirs and Seed (1969) compared simple shear and triaxial compression test data by plotting static normalized stress-strain curves as shown in Figure 8. Simple shear tests were carried out with the shear stresses applied to a horizontal sediment plane, whereas triaxial tests were conducted on specimens extracted at various orientations with respect to the sediment layering so as to be loaded at various angles β from the vertical sediment direction. This figure shows that at lower stress levels, all triaxial plots agree very well with the simple shear results; but, at higher stresses and at failure, triaxial tests give lower values of strain.

Thiers and Seed (1969) carried out several investigations on the cyclic stress-strain behavior of saturated clays. For comparison with static behavior, results were plotted in the nondimensional form of the dynamic modulus ratio (dynamic modulus divided by static modulus) against the cyclic strain ratio (peak cyclic strain divided by failure strain), as shown in Figure 9. In this figure most of the changes in the modulus ratio lie in the first 50 cycles. Similarly, Thiers and Seed (1969) plotted the ratio of yield strain to failure strain against the cyclic strain ratio for clay samples shown in Figure 10. Here, the plot is, relatively, a linear strain relationship up to a value of about unity for the cyclic strain ratio, after which the yield strain ratio rapidly increases to a value of 0.45, corresponding to a value of cyclic strain ratio of 1.5, which is an increase of about four times the previously attained value.

These soil stress-strain data obtained by various authors give an indication of what may be expected from seafloor soils under dynamic loading. The data indicate that most seafloor soils would tend to be quite susceptible to large cyclic stress levels resulting in large soil deformations in the direction of sustained loading, thus permitting an embedded anchor to displace upward and causing it to eventually pull out.

Loss of Strength and Liquefaction. A granular soil may lose its strength when its fabric is disturbed, either by vibration or by shearing. In the seafloor soils of oceanic trenches, for example, disturbance caused by the strong vibrations of frequent earthquakes, will change interparticle orientations and contact stresses.

The term "liquefaction" implies a reduction in the resistance of the sediment to deformation from that of a plastic solid, having a measurable shear strength, to that of a liquid, having only a viscous resistance to flow. Liquefaction will periodically break up the contacts between the sediment particles, creating frequently redeposited

turbidite beds in which the particles do not become strongly cemented. In contrast, some granular pelagic sediments, such as calcareous oozes, that are not in an earthquake zone may acquire a considerable amount of strength as a result of interparticle cementing. Vibrations would therefore be more likely to liquefy granular turbidite beds than cemented pelagic sediments.

On a geological time scale, liquefaction of seafloor soils will be a frequent, but transient, occurrence at any particular place. Several months or years may pass without any liquefaction occurring; on the other hand, at much longer intervals very large earthquakes will induce widespread liquefaction lasting up to half a minute or more, depending upon the thickness and the permiability of the sedimentary layer involved.

In cohesive soils, the same disturbance phenomeon occurs, but the cohesive strength component in the soil restricts the effects to a partial strength loss, rather than a complete liquefaction. Soil strength reduction has been investigated by several researchers on different types of soils under cyclic loading, as subsequently described.

The dynamic behavior of cohesive seafloor soils should be closely related to that of some terrigenous muds because of similar static soil properties and soil composition. The dynamic behavior of one such soil has been determined by Seed and Chan (1966)- San Francisco Bay mud. In Figure 11 are summarized many of the test results obtained during this study. In this figure, relationships are given between the sustained and pulsating stress levels that produce failure for various selected numbers of stress applications. The plotted lines indicate the stress state (in terms of sustained and pulsating stresses normalized by the static undrained strength) at which failure will occur following a specified number of transient stress pulses. As may be seen, the worst situation investigated is that in which there is no sustained stress and the number of transient load applications is 900, corresponding to a pulsating stress of about 60% of the normal strength.

Cyclic loading has been found to have a small effect on the static strength immediately after cessation of the cyclic loading. As shown in Figure 12 (Thiers and Seed, 1969), the loss of strength for San Francisco Bay mud samples were found to be very little. Even after 200 strain cycles and at a cyclic shear strain (amplitude) of 2% to 3%, the soil strength was only reduced by 10%. Below a cyclic shear strain of 1.5%, the soil was virtually unaffected by 200 cycles of straining.

A cyclic strength decrease factor has been given by Thiers and Seed (1969) for cohesive soils in a plot between the strength ratio (strength after cyclic loading over original strength) versus the cyclic strain ratio (cyclic strain over failure strain in the static test) Figure 13. This normalized plot shows only small reductions in strength for cyclic strain ratios less than 0.4 but rather drastic reductions for ratios greater than 0.6. For design work it would be quite suitable to limit loading magnitudes so as to limit the cyclic strain ratio to

values less than 0.5. This would limit strength loss to less than 20% of the original strength, after 200 strain cycles.

Increases in the resistance of soils to liquefaction have been observed after an initial liquefaction and settling period (Lee and Focht, 1975a, Finn et al., 1970a). These increases are probably caused by better interlocking of the particles than in the original structure, before the cyclic loading was applied. Thus, the soil stress history plays an important role in the resistance of the soil to liquefaction under cyclic loading.

The cyclic shearing strength expressed as a percentage of the static undrained strength for several different types of clay soils is illustrated in Figure 14 (Lee and Focht, 1975b). Within the plotted range of variation of cyclic soil strength ratio versus number of cycles for all soils considered, the seafloor soils are not restricted to a smaller range, but fall near the upper and lower limits as well as in between. The cyclic strength ratio for 100 cycles to failure varied from about 15% for the North Sea soil samples up to about 65% for the Ekofisk sandy clay which is also in the North Sea.

Soil strength at a given density may differ considerably under cyclic loading, depending on the soil's particle sizes. Lee and Fitton (1969) compared the cyclic strength of eight different soils subjected to the same confining pressure (σ_3 = 15 psi). As shown in Figure 15, the cyclic strength of silty clay is found to be three times greater than for silt and sandy soils having grain sizes down to nearly those of the silty clay, thus suggesting that the grain size may not be the only factor governing the soil strength, but that the soil plasticity may also be of considerable importance. The above discussion indicates that seafloor soils tend to have a wide range of soil strength under cyclic loading, depending on the density, depositional environment, cementation, particle size, composition, plasticity, and stress history.

Shock Loading and Slow Loading. When shock loads are applied to a soil, its response reflects inertially induced stresses as well as the cyclic loading effects previously discussed. On the other hand, when transient loads are applied slowly, there is time for drainage to occur, so that the building of pore pressure will be reduced and the effects of cyclic loading on strength reduction will be mitigated. Analytical methods for accounting for these effects are being finalized at CEL and will be published soon (Gouda, 1976).

Anchor Parameters

The holding capacity of an embedment anchor depends mainly on the following anchor parameters:

(a) Depth of embedment
(b) Buoyant weight of anchor
(c) Angle of line pull
(d) Size and shape of the anchor fluke

Other parameters of significant importance for consideration depend on the type of anchors used (Beard and Lee, 1975). For the CEL propellant-actuated deep water embedment anchors, the flat-plate configuration promotes the establishment of soil suction forces beneath the anchor fluke; hence, the tendency of a shape to promote such suction is an important parameter.

Another important parameter is disturbance (Rocker, 1977). The fluke disturbs soil during penetration, by the passage of the leading edges of the anchor plate and any protrusions. The shape and texture of these edges affect the amount and extent of disturbance. The disturbed soil increases the pulling distance required to set the anchor fluke, resulting in a reduced capacity if the anchor is pulled to a shallower, weaker sediment layer. Once the fluke is set, the relatively small zone of disturbed soil appears to have only a small effect on holding capacity.

Environmental Parameters

Environmental parameters may influence the loading of an anchor or foundation and the capability of the supporting soil to sustain that loading. Environmental parameters affecting load are discussed in the following section.

There are several environmental characteristics which might influence the soil behavior. The two most significant parameters are the pore fluid composition and the temperature.

Pore Fluid. Occasionally, a submerged marine clay is encountered that has a history of being previously uplifted above sea level. When such a clay was uplifted, the ground water percolating through the clay was of much lower salt content than seawater (35 grams of salt per liter of water). Thus, during the life of a "marine" clay there might occur a removal of the salt in the pore fluid. This leaching would cause damage in interparticle forces and overall properties that would, in turn, cause the sediment to behave differently from a nonuplifted sediment, even after it resubmerged and salt was reintroduced into the pore fluid. Also, soluble elements in the deposited soil might dissolve, raising the concentration in the pore fluid of certain ions and compounds (notably calcium, magnesium, iron, carbonate, sulfate, and silica). Changes in the concentration of solutes in the pore fluid can affect the shear strength of the soil.

Temperature. Changes in temperature act on the soil to produce changes in soil strength and response rate and can cause errors in dynamic, static, and index test measurements. A seafloor temperature is typically in the vicinity of 4°C. When laboratory tests are conducted on a soil sample, the temperature may increase up to 25°C or more. If proper precautions are not taken, such a rise in temperature would cause pore water expansion on the order of 0.5%, resulting in an expansion of the soil and an accompanying decrease in soil strength. Also, creep

rate increases with increasing temperature. On the other hand, calcium carbonate precipitates as temperature increases, creating bonds that increase the strength of soils having pore fluids that are already saturated with calcium carbonate. Because a proper accounting for all of these effects is difficult, it is highly advisable to maintain the in situ temperature during the handling, storage, and testing of seafloor soil samples.

Load Parameters

Dynamic load parameters differ according to the type of loading. In the following paragraphs, predominant types of dynamic loading are given with a brief outline of their relationship to cyclic soil behavior. This information is summarized in Table 3.

Rapid Cyclic Loading (With Inertial Forces).

(1) Earthquake Loads. During an earthquake an element of a soil mass is subjected to a series of alternating shear stresses which vary in magnitude in a somewhat random fashion. Vertical and horizontal inertial forces are created along with the initial overburden stresses; these inertial forces tend to increase the soil's pore pressure progressively. This can lead eventually to the sudden loss of strength known as liquefaction.

(2) Vortex Shedding (Cable Strumming). The magnitude of the dynamic load increment caused by cable strumming is related to the current velocity and the cable characteristics. A theoretical method is presented in Appendix A for use in making rough predictions of load magnitude and frequency.

Slow Cyclic Loading (Without Inertial Forces).

(1) Wave Loads. Soil may be loaded by waves directly, as they apply varying hydrostatic pressure to the seafloor (shallow water only) or indirectly, as they apply oscillatory forces to a moored object. The possibility of ocean waves producing liquefaction in sandy silt seafloor soils is somewhat similar to the problem of earthquake-induced liquefaction of soils. However, ocean wave excitation differs from earthquake excitation in three major aspects:

(a) The storm waves have periods considerably longer than earthquake loading.

(b) The duration of an ocean storm is significantly longer than that of an earthquake.

(c) The probability that a structure in the ocean would be subjected to storm waves is much higher than for earthquakes.

Dynamic testing of soils for the analysis of ocean wave loading effects should be performed under a cyclic frequency of approximately 1 cycle every 6 to 12 seconds, which corresponds to the larger typical

ocean storm waves. Use of cyclic tests conducted at higher frequencies may be feasible; however, it is not presently known how to account for the effects of the increased drainage occurring between less frequent pulses.

(2) Current Fluctuations. For most installations in soils of low permeability, diurnal or other fluctuations in current will occur slowly enough that the soil will respond with partial drainage. The magnitude of soil loading fluctuations caused by current fluctuations will be small relative to other types of cyclic loading in most instances. When required, predictions of behavior under these conditions may be made analytically from a knowledge of the response of similar soils to more rapid cyclic loading, by accounting for the effects of drainage in reducing the buildup of excess pore pressures.

Shock Loading. Shock loading may be produced by blast, impact, or line snap loads.

(1) Blast Loads. An underwater blast may load a moored object, the mooring line, the seafloor soil, and the embedded anchor. Such loads are of short duration for conventional explosions but may endure for large fractions of a second for nuclear blasts. Blast loading effects should be analyzed by considering inertia and undrained soil response during a single pulse.

The effects of repeated blasts may be analyzed by considering the soil's incomplete dissipation of pore pressure changes between successive pulses.

(2) Impact and Line Snap Loads. Motion of the moored object may cause a slack line to be pulled straight abruptly, leading to sharp increases in line loading. This is termed line snap. Similar sharp loads may be caused by impactive loading of the moored object. Such loads should be considered on a case-by-case basis. The number of cycles and level of dynamic load increment will depend upon the type of installation and the source of external loading or the motion-inducing environment. The soil will respond in an undrained state but may have time for drainage (partial or complete) between impacts. Inertial forces must be considered.

AVAILABLE TESTING TECHNIQUES

The laboratory tests available for measuring the dynamic mechanical properties of soils directly are listed below, along with references describing their use.

Cyclic simple shear test
- Peacock and Seed (1968)
- Finn et al., (1971)

Cyclic torsional shear test
Ishihara and Li (1972)

Cyclic torsional simple shear test
Ishibashi and Sherif (1974)

Cyclic triaxial shear test
Seed and Lee (1966)

Resonant column test
Wilson and Dietrich (1960)
Hardin and Richart (1963)
Hardin and Music (1965)
Drnevich et al., (1967)

Shake table test
Finn et al., (1970b)

Resonant column testing has become a common laboratory procedure but is limited in relation to dynamic soil properties. Its primary drawback is that it can be used only for low shear strain amplitudes. Therefore, it is limited to certain types of dynamic soil testing.

The cyclic simple shear test, although it can yield reliable data when conducted properly, still has deficiencies which include a large amount of wall friction and an inability, in the circular configuration, to control or measure the effective horizontal stresses. Moreover, the cyclic simple shear testing device does not produce uniform shear stresses throughout the soil sample.

Cyclic torsional testing devices (simple shear or triaxial) are still fairly new, and research work is still needed to verify their dynamic results. They are limited to certain soil sample sizes and shapes and to a preparation method which is not common in engineering practice.

Finally, the cyclic triaxial testing device is believed to be the most practical testing device for present application for the following reasons:

(1) The test is simple to perform, and the equipment is widely available at moderate cost.

(2) Comparisons of dynamic results with field performance indicate that cyclic triaxial test data provide a useful basis for evaluating liquefaction potential in the field, although the cyclic shear stresses causing liquefaction obtained by the testing device should be reduced by 30% to yield conservative predictions of stresses causing liquefaction in the field.

(3) The cyclic triaxial testing device has been used extensively by several researchers with very reliable and repeatable results.

INTERIM DESIGN METHODS

General Approach

In this section, interim methods are given for carrying out specified design steps. They are recommended for use until more efficient methods are developed from the results of ongoing research.

It is expected that future methods will be formulated as extensions and refinements to the present design methods. Ongoing research includes the detailed analysis of soil stresses around anchors to determine their effects on relationships between anchor loading and response. These relationships will be used to develop improved design methods formulated around the present single-degree-of-freedom idealization, so that the user will have to consider only the overall relationships (but not the stresses on individual soil elements).

A reasonable approach to the prediction of anchor behavior for design purposes includes the following steps:

(1) The applied loads from the sources mentioned previously (LOAD PARAMETERS section) are separated into components, and each cyclic component is characterized in terms of magnitude and frequency.

(2) The overall interactions between the loading components and the system are assessed in order to evaluate dynamic load magnification and effective damping.

(3) The magnified system loads are expressed in terms of stresses on soil elements.

(4) The responses of soil elements to the conditions imposed on them are determined from knowledge of soil behavior, including creep, drainage, and liquefaction or partial strength loss under dynamic loading.

(5) The response of the system is expressed in terms of soil element responses. Any changes in system response affecting overall load-system interaction are used to correct the dynamic load magnifications and load-stress relationships iteratively. Predictions are continued until the loading and the resulting responses (including long-term responses, such as creep), are completed, or until failure occurs.

Line Loads

A dynamic line load is resolved into static, cyclic, stepped, and impact components. The cyclic components are characterized in terms of magnitude and frequency. The probability of occurrence of each component may be evaluated so that an overall probability of failure may be determined for the anchored system after the failure effects of the loading components are determined.

With this idealization, the cable and anchor normally will be stiff relative to the soil, so that most of the resiliency and dampening in the system will come from the soil surrounding the anchor. As this soil

will fail under excessive strains, low to moderate levels of strain are sought (depending upon the number of loading cyclic anticipated for the life of the system). A low-value damping factor -- say 0.02 to 0.05 -- would result. A soil mass equal to that contained in the smallest sphere (for a circular or square plate) or ellipsoid (for a rectangular plate) surrounding the anchor acts in concert with the anchor and cable mass. The system should be analyzed to obtain dynamic load factors for the dynamic loading frequencies of concern, which should be multiplied by the magnitudes of those dynamic loads. The sum of these products and the static load is the total design load.

The anchor, soil, and cable are first incorporated into a lumped mass model (spring-mass-damper system); the anchor and its cable are the total mass of the system and the damping carried by the surrounding soil. Hence, the motion of the anchor during dynamic loading may be approximated by rigid body motion (see Figure 16). The side frictional force is assumed to be equal to zero; its effect (if any) may be incorporated with the suction force. The suction force is usually very high at the initial displacement, tending to decrease with the decrease of embedment depth. The total suction force along the bottom side of the anchor fluke will be determined from Figure 6 for the relative embedment depth ratio of concern.

The net soil dynamic resistance force $F_r(t)$ is equal to the difference betewen the applied anchor load and the sum of the suction force and the total inertial force, as

$$F_r(t) = F_t(t) - F_s(t) - M\,\ddot{z}(t) \qquad (1)$$

where $F_r(t)$ = total uplift force (static plus dynamic)

$F_s(t)$ = total suction force along the bottomside of the fluke

M = total mass of anchor plus cable plus oscillating soil

$\ddot{z}(t)$ = measured acceleration

For static loading, the holding capacity has been given by Taylor and Lee (1972) as

$$H_s = A_f\,(c\bar{N}_c + \gamma_b\,D\,\bar{N}_q)\,(0.84 + 0.16\,B/L) \qquad (2)$$

where A_f = fluke plan area (ft^2)

c = unit soil cohesion (psf)

γ_b = buoyant unit weight of soil (pcf)

D = fluke embedment depth (ft)

B = fluke diameter or width (ft)

L = fluke length (ft)

$\overline{N}_c$ & $\overline{N}_q$ = Holding capacity factors that depend on the type of loading, soil type and density, and the relative embedment depth (D/B)

Values of $\overline{N}_c$ and $\overline{N}_q$ are given in Figure 17 for cohesive and noncohesive soils. For further details, including methods for determining the required parameters, the reader is referred to the "Handbook for uplift-Resisting Anchors" by R. Taylor et al, Sep 1975.

Equation 2 accounts for the effects of the soil's resistance to deformation under the application of stresses by an upwardly applied anchor line load. However, for dynamic loading, the effects of repeated load application on soil strength and the effects of inertia on loading also must be accounted for.

The effects of the inertia of the anchor, mooring, and soil acting as a single-degree-of-freedom system may be treated by lumping moving masses, with the soil mass equal to an "effective" value given by the mass of soil enclosed by a sphere or ellipsoid surrounding a circular, square, or rectangular anchor plate. As discussed in Appendixes B, C, and D, these effects might result in significant load magnifications for some occasionally encountered conditions, but should produce a dynamic response equal to the quasi-static response to the peak dynamic load for a majority of typical mooring requirements.

The effects of repeated loading on the soil surrounding an anchor are best analyzed by considering the responses of soil elements to static loading and then determining how they change when the loading is not static. The soil's resistance to deformation that gives rise to the holding capacity given by Equation 2 may be broken down into element resistances by finite element analysis in a manner similar to that employed by Beard (1974), for example. Typical stresses are shown in Figures 18 and 19; these figures may be used as a guide for interpolation to obtain rough estimates. The same relationships between load and stress may be used to estimate both the static and the dynamic components of stress at various points around the anchor.

The soil response to stresses determined as discussed above may be obtained by using data such as that presented in Figure 11. However, for common seafloor soils, results of more recent studies (Herrmann and Houston, 1976) may be utilized. These studies showed that an often-critical condition exists in a region where the static component of shear stress is low, thus permitting shear stress reversal even when the magnitude of the dynamic component is low. Such a region exists beneath an upward-loaded anchor plate as a result of the combined effects of sediment overburden stresses and anchor-induced stresses. The reduced soil strengths in various regions around the anchor should be used in an equilibrium equation involving the overall load, in order to determine the corresponding increase in stresses in other regions, for use in the subsequent iterative determination of soil response. As this redistribution causes a reduction in system stiffness, the subsequent

iteration also involves the re-examination of dynamic load factors, as discussed in Appendixes B, C, and D. The iteration process eventually will lead to the prediction of failure if the selected anchor is smaller than the sought critical size for the considered mooring and earthquake loads.

Sediment Loads

The soil surrounding a loaded embedment anchor is a part of the overall load-transmitting system. As such, this soil is loaded by the remainder of the sediment around and above it. In addition to static overburden loading, dynamic loads may be induced by wave action, a nearby blast, an earthquake, or other environmental disturbances. The wavelengths of such loadings are large in comparison to the size of an anchor; hence, the situation may be idealized as a rigid anchor in a medium that is not distorted by the loading waves, but only by the relative motion of the anchor.

The sediment load produces (1) soil stresses throughout the soil by internal waves that arise from soil inertia and (2) higher soil stresses in the soil around the anchor because the total effective mass of the anchor and any connected masses is different (usually larger) than the mass of the displaced soil. The combined dynamic and static stresses influence soil behavior and hence anchor performance.

Free-field soil stresses induced by sediment loading may be calculated by using conventional relationships of static and wave mechanics. The stresses induced in the soil surrounding a loaded anchor may be calculated on the basis of a single-degree-of-freedom idealization, by first determining the effective anchor load as the product of the effective mass and acceleration of the soil medium caused by the sediment loading, and then quasi-statically determining stresses from relationships such as those depicted in Figures 18 and 19. Dynamic load magnification considerations are included in this idealization. The resulting stresses would then be used to determine the dynamic response of the soil in the same way as for line-load-induced stresses.

Earthquake Loads

Earthquakes have a potential for loading an anchor line and the sediment simultaneously. The determination of the response of an anchor during an earthquake involves the following steps:

(1) The magnitudes and phasing of line loads are determined from the earthquake intensity with respect to the moored mass, orientation, and configuration of the mooring.

(2) The magnitudes and phasing of sediment motions and the resulting effective inertial loads on the anchor are determined from the intensity and direction of the earthquake shaking at the site.

(3) The combined effects on soil stresses are determined from vector sums of the combined dynamic and static loads in various potentially critical directions, using the quasi-static load-stress relationships.

(4) The soil response to the applied stresses, the resulting system response, and feedback effects are determined in a way similar to that used for a line load or a sediment load acting alone.

It is noted that the resonance effects leading to possible dynamic load magnification are included in the single-degree-of-freedom idealizations required in steps (1) and (2). Although this procedure involves a linear superposition of effects, several iterations through the steps involving dynamic load magnification, stress determination, and dynamic soil response should yield results that account for the nonlinear interactions of these factors.

Design Features for Reducing Dynamic Effects

The effect of additional dynamic line loads may be eliminated or reduced by using shock-abosrbing elements in the line that will tend to dissipate the dynamic force and thus allow only small load variations to reach the embedded anchor fluke. The effect of such elements in reducing load variations is easily accounted for in design calculations. Reductions will be more pronounced for higher-frequency dynamic loadings. As an example, a section of synthetic line (low modulus) between the anchor and the bulk of the mooring line (high modulus) would reduce to an insignificant level the magnitude of strumming-induced axial force oscillations reaching the anchor.

Analytical Example

Basis. In the following example, steps are carried out for determining whether or not a proposed anchor is safe. A comprehensive procedure based upon the aforementioned approach, consists of the following steps:

(1) Design parameters are stated.

(2) The relative embedment depth is determined.

(3) The type of soil is identified.

(4) The soil's undrained shearing strength is determined.

(5) The dynamic soil shearing strength is determined from an assumed ratio of loading to failure strain.

(6) The holding capacity factors $\bar{N}_c$ and $\bar{N}_q$ are determined.

(7) The quasi-static anchor holding capacity is determined from equation 2.

(8) The total holding capacity is determined considering the dynamic effects described in Appendixes B, C, and D.

(9) If the resulting load-to-capacity strain ratio exceeds that assumed in step 5, a further iteration of step 5 through 9 is needed.

Also, the dynamic effects described in Appendixes B, C, and D (step 8) are affected by strain.

A simplified procedure is warranted in many cases. The dynamic soil shearing strength is assumed to be less than the static strength by 20% as long as the cyclic strains are limited to less than half of the static failure strain. As the applied anchor loads are slow in comparison with the natural frequency of the moored system, the total anchor holding capacity (H_T) can be determined without considering the dynamic load magnifications described in Appendixes B, C, and D.

The example given below is limited to this simplified procedure.

Supposition. A direct embedment anchor with a 3-ft-diam fluke is to be embedded in stiff clay soil up to a depth of 10 feet. The anchor is to hold a surface buoy in position for several years. Figure 20 gives a vane shear strength profile for the type of seafloor encountered. The buoyant unit weight is stipulated to be 35 pcf throughout the soil profile, with the soil sensitivity equal to two. The anchor holding capacity (combined static and dynamic) is to be determined for the following conditions.

Mooring Characteristics:

Water Depth, W.D. = 50 ft

Cable Length, Lc = 150 ft

Scope, $\frac{L_c}{W.D.}$ = 1.5

Storm Condition:

A severe storm is assumed. The equivalent cyclic plus static peak load is stipulated to be 2,000 pounds at 0.1 Hz, occurring for a total of 75 days on the average during a 3-year period.

Solution.

(1) Design parameters are stated as follows:

$$D = 10 \text{ ft}$$

$$B = 3 \text{ ft}$$

$$L = 3 \text{ ft}$$

$$A_f = 7.06 \text{ ft}^2$$

$$\gamma_b = 35 \text{ pcf}$$

(2) The relative embedment depth is determined:

$$D/B = 10/3 = 3.3$$

(3) The type of soil is identified as a stiff clay soil (cohesive soil).

(4) The soil's undrained shearing strength is determined from the given vane shear strength profile (Figure 20) at the given depth of embedment (10 ft):

$$S_u = 338 \text{ psf} = 2.35 \text{ psi}$$

(5) The dynamic soil shearing strength is determined. For dynamically loaded soils, if the cyclic strains are limited to less than half of the static failure strain, the soil static strength value S_u will be reduced by 20% at most (see Figure 13). Therefore, the dynamic soil shear strength is:

$$S_D = 270 \text{ psf} = 1.9 \text{ psi}$$

(6) The holding capacity factors $\bar{N}_c$ and $\bar{N}_q$ are determined for

$$c = S_D = 1.9 \text{ psi}$$
$$D/B = 3.3$$
$$\phi = 0 \text{ deg}$$

From Figures 17a and 17b:

$$\bar{N}_c = 8.0$$
$$\bar{N}_q = 1.0$$

(7) The quasi-static anchor holding capacity is determined from Equation 2:

$$H_s = A_f \ (c \bar{N}_c + \gamma_b \ D \bar{N}_q) \ (0.84 + 0.16 \ B/L)$$
$$= 7.06 \ (270 \times 8 + 35 \times 10 \times 1) \ (0.84 + 0.16 \times 3.3)$$
$$= 17{,}740 \text{ lb}$$

(8) The total holding capacity H_T is determined. As the applications of load are slow in comparison with the natural frequency of the moored system, no dynamic load magnifications are expected. Hence,

$$H_T = H_s = 17{,}740 \text{ lb}$$

(9) The total holding capacity is compared with the expected load.

$$H_T = 17{,}740 \text{ lb} > 2{,}000 \text{ lb (due to wave force)}$$

Hence, the anchor is predicted to hold. As the dynamic capacity, computed from the assumptions made in steps 5 and 8, is very much higher than the loading, the assumptions are on the conservative side, and no further iterations are necessary.

CONCLUSIONS

The conclusions of this study are as follows:

(1) The static and dynamic soil parameters relevant to the holding capacity of deeply embedded propellant-actuated anchors, are the soil moduli, creep, suction, cyclic strength loss, stress-strain relationships under dynamic loading, and responses to shock and slow loading. Also, environmental parameters of soil pore fluid composition and temperature that are unrelated to load affect soil properties.

(2) The anchor-related parameters in the anchor-soil-load-environment system relevant to holding capacity are (a) the anchor embedment depth, buoyant weight, angle-of-line pull, and size and shape of fluke; and (b) magnitudes of the static and dynamic components of loading and the dynamic loading period for loads produced in the line by current fluctuations, waves, vortex shedding, impact, or line snap and for loads produced more or less simultaneiously in the line and the sediment by earthquakes or underwater blasts.

(3) Of the available dynamic test methods, the cyclic triaxial test is recommended for determining the response of soils to the stress conditions that would occur around a dynamically loaded embedment anchor.*

(4) The derived design method for determining the dynamic holding capacity of embedment anchors is suitable for interim use by design engineers. It is expected that this method will be refined following the completion of current research on seafloor soils. The example given at the end of "Interim Design Methods" demonstrates the use of this method and provides the user with insight into the assumptions required to evaluate the pertinent factors and parameters.

RECOMMENDATIONS

It is recommended that the design guidelines given in this report be used in seafloor engineering involving dynamic loading (particularly

*Knowledge of cyclically loaded soil response may be extended to slow loading and shock loading by using the results of current CEL work that will be published in the near future.

in the engineering of embedment anchors to sustain dynamic loading) until improved versions are developed. Field data from dynamically loaded embedment anchor moorings in actual use and other operating seafloor structures should be collected over extended periods of time for use in verifying and refining the presently available design methods.

FUTURE RESEARCH

Dynamic and static tests of anchors embedded at selected seafloor sites will be conducted along with extensive investigations of the sediment properties to provide data in greater detail. These data will be used together with results of current soil property tests, model anchor tests, and mathematical modeling studies to refine the simplified lumped mass model described in this report, and to refine the inputs to that model used to represent the relevant sediment properties. The results of this work, which will supersede the guidelines reported here, will be promulgated in a final report that should be available in 1978.

REFERENCES

Adams, J.I. and Hayes, D.C. (1967) "The uplift capacity of shallow foundations," Ontario Hydro Research Quarterly, vol 19, no. 1, 1967.

Aisiks, E.G. and Tarshansky, I.W. (1969) "Soil studies for seismic design of San Francisco transbay tube," in Proceedings of Symposium of the Seventy-first Annual Meeting of the American Society for Testing Materials, San Francisco, Calif., Jun 1968. New York, N.Y., American Society for Testing Materials, 1969. (ASTM Special Technical Publication STP-450).

Ali, M.S. (1968) "Pullout resistance of anchor plates and anchor piles in soft bentonite clay", M.S. thesis, Duke University. Durham, N.C., 1968.

Beard, R.M. (1974) Status report: Development of an expedient site investigation tool and investigations in long-term anchor holding capacity, Civil Engineering Laboratory Letter Report. Port Hueneme, Calif., May 1974.

Beard, R.M. and Lee, H.J. (1975) "Holding capacity of direct embedment anchors", in Proceedings of Civil Engineering in the Oceans--III, vol 1, New York, N.Y., American Society of Civil Engineers, Jun 1975, pp 470-485.

Bishop, A.W. (1971) "Shear strength parameters for undistributed and remoulded soil specimens; stress-strain behavior of soils", in Proceedings of the Roscoe Memorial Symposium, Cambridge University, 29-31 Mar 1971, pp 35-44.

Davisson, M.T. (1965) "Static and dynamic behavior of sands in one dimensional compression", Air Force Weapons Laboratory, Technical Report no. AFWL-TR-65-29. Kirtland Air Force Base, N.M., Dec 1965.

Drnevich, V.P., Hall, J.R., Jr. and Richart, F.E., Jr. (1967) "Effects of amplitude of vibration on the shear modulus of sands", in Proceedings of the International Symposium on Wave Propagation and Dynamic Properties of Earth Materials, Albuquerque, N.M., Aug 1967. Albuquerque, N.M., ASCE National Science Foundation, University of New Mexico Press, Aug 1968.

Finn, W.D.L., Bransby, L. and Pickering, J. (1970a) "Effect of strain history on liquefaction of sand", Journal of the Soil Mechanics and Foundation Division, ASCE, vol 96, no. SM6, Nov 1970, pp 1917-1934. (Proc. Paper 7670)

Finn, W.D.L., Emery, J.J. and Gupta, Y.P. (1970b) "A shaking table study of the liquefaction of saturated sands during earthquakes", in Proceedings of the Third European Symposium on Earthquake Engineering, Sofia, Bulgaria, Sep 1970, pp 253-262.

Finn, W.D.L., Pickering, D.J. and Bransby, P.L. (1971) "Sand liquefaction in triaxial and simple shear tests", Journal of the Soil Mechanics and Foundations Division, ASCE, vol 97, no. SM4, Apr 1971, pp 639-659. (Proc. Paper 8039)

Gouda, Z.M. (1977) "An analytical study of anchor response to shock and slow loads", Civil Engineering Laboratory, Technical Memorandum (to be published).

Hardin, B.O. and Drnevich, V.P. (1970) Shear and modulus and damping in soils: I. Measurement and parameter effects, II. Design equations and curves, University of Kentucky, College of Engineering, Technical Report UKY 27-70-CE 2 and 3. Lexington, Ky., Jul 1970.

Hardin, B.O. and Drnevich, F.P. (1972) "Shear modulus and damping in soils, design equations and curves", Journal of the Soil Mechanics and Foundations Division, ASCE, vol 98, no. SM7, Jul 1972, pp 667-691.

Hardin, B.O. and Music, J. (1965) "Apparatus for vibration during the triaxial test", in Proceedings of the Symposium on Instrumentation and Apparatus for Soils and Rocks, Lafayette, Ind., 13-18 Jun 1965. Philadelphia, Pa., ASTM 1965. (ASTM STP no. 392)

Hardin, B.O. and Richart, F.E., Jr. (1963) "Elastic wave velocities in granular soils", Journal of Soil Mechanics and Foundations Division, ASCE, vol 89, no. SM1, Feb 1963, pp 33-65.

Herrmann, H.G. and Houston, W.N. (1976) "Response of seafloor soils to combined static and cyclic loading", in Proceedings of 1976 Offshore Technology Conference, Houston, Tex., May 1976. Houston, Tex., American Society of Civil Engineers, 1976. (Paper no. OTC 2428)

Holzer, T.L. and Hoeg, K. (1973) "Effect of seismic loading on undrained clay creep", Journal of the Soil Mechanics and Foundations Division, ASCE, vol 199, no. SM1, Jan 1973, pp 153-158.

Ishibashi, I. and Sherif, M.A. (1974) "Soil liquefaction by torsional simple shear device", Journal of the Geotechnical Engineering Division, ASCE, vol 100, no. GT8, Aug 1974, pp 871-883. (Paper 10752)

Ishihara, K. and Li, S. (1972) "Liquefaction of saturated sand in triaxial torsion shear test", Soils and Foundations, (Japan), vol 12, no. 3, Jun 1972, pp 19-39.

Lee, H.J. (1973) In-situ strength of seafloor soil determined from tests on partially disturbed cores, Naval Civil Engineering Laboratory, Technical Note TN-1295. Port Hueneme, Calif., Aug 1973.

Lee, K.L., Seed, H.B. (1964) "Pulsating Loading Tests on Samples of Fine Silty Sand from Anchorage, Alaska", Appendix C, Report on Anchorage Area Soil studies to U.S. Army Engineer District, Anchorage, Alaska, Shannon and Wilson, Inc., Seattle, Washington, Aug 1964.

Lee, K.L. and Fitton, J.A. (1969) "Factors affecting the cyclic loading strength of soil", in Proceedings of Symposium of the Seventy-first Annual Meeting of the American Society for Testing Materials, San Francisco, Calif., Jun 1968. New York, N.Y., ASTM, 1969. (ASTM STP-450)

Lee, K.L. and Focht, J.A. (1975a) "Liquefaction potential in the North Sea", Journal of the Geotechnical Engineering Division, ASCE, vol 101, no. GT1, Jan 1975, pp 1-18. (Proc. paper no. 11054)

Lee, K.L. and Focht, J.A. (1975b) "Strength of clay subjected to cyclic loading", in Proceedings of Speciality Conference on Civil Engineering in the Ocean, University of Delaware, Newark, Del., Jun 1975.

Lysmer, J. and Richart, F.E., Jr. (1966) "Dynamic response of footings to vertical loading", Journal of the Soil Mechanics and Foundations Division, ASCE, vol 92, no. SM1, Jan 1966, pp 65-91.

Mayerhof, G.G. and Adams, J.I. (1968) "The ultimate uplift capacity of foundations", Canadian Geotechnical Journal, vol 5, no. 4, Nov 1968, pp 225-244.

Peacock, W.H. and Seed, H.B. (1968) "Sand liquefaction under cyclic loading simple shear conditions", Journal of the Soil Mechanics and Foundations Division, ASCE, vol 94, no. SM3, May 1968, pp 689-708.

Richart, F.E., Jr., Hall, J.R., Jr. and Woods, R.D. (1970) Vibrations of soils and foundations. Englewood Cliffs, N.J., Prentice-Hall, Inc., 1970.

Rocker, J., Jr. (1977) "The effects of sediment penetration on embedment anchor holding capacity", Civil Engineering Laboratory, Port Hueneme, Calif., (to be published).

Seed, H.B. (1968) "Landslides during earthquakes due to soil liquefaction, Fourth Terzaghi Lecture", Journal of the Soil Mechanics and Foundations Division, ASCE, vol 94, no. SM5, Sep 1968, pp 1053-1122.

Seed, H.B. and Chan, C.K. (1966) "Clay strength under earthquake loading conditions", Journal of the Soil Mechanics and Foundations Division, ASCE, vol 92, SM2, Mar 1966, pp 53-78. (Proc. Paper 4723)

Seed, H.B. and Idriss, I.M. (1970) "Soil moduli and damping factors for dynamic response analysis", University of California, College of Engineering, Report no. EERC 70-10. Berkeley, Calif., Dec 1970.

Seed, H.B. and Lee, L.L. (1966) "Liquefaction of saturated sands under seismic loading", Journal of Soil Mechanics and Foundations Division, ASCE, vol 95, no. SM5, Sep 1966, pp 1199-1218.

Singh, A. and Michell, J.K. (1968) "General stress-strain-time function for soils", Journal of Soil Mechanics and Foundations Division, ASCE, vol 94, no. SM1, Jan 1968, pp 21-46. (Prop. Paper 5728)

Taylor, R.J. (1976) "CEL 20K propellant actuated anchor", Civil Engineering Laboratory, Technical Report R-837. Port Hueneme, Calif., Mar 1976.

Taylor, R.J., Jones, D. and Beard, R.M. (1975) "Handbook for uplift-resisting anchors", Civil Engineering Laboratory. Port Hueneme, Calif., Sep 1975.

Taylor, R.J. and Lee, H.J. (1972) "Direct embedment anchor holding capacity", Naval Civil Engineering Laboratory, Technical Note TN-1245. Port Hueneme, Calif., Dec 1972.

Thiers, G.R. (1965) "The behavior of saturated clay under seismic loading conditions", Ph.D. thesis, University of California. Berkeley, Calif., 1965.

Thiers, G.R. and Seed, H.B. (1969) "Strength and stress-strain characteristics of clays subjected to seismic loading conditions", in Proceedings of Symposium of the Seventy-first Annual Meeting of the American Society for Testing Materials, San Francisco, Calif., Jun 1968. New York, N.Y., American Society of Testing Materials, 1969, pp 3-56. (ASTM STP-450)

True, D.G. and Taylor, R.J. (1975) CEL 100K propellant anchor - utilization for tanker moorings in soft coral at Diego Garcia, Civil Engineering Laboratory, Technical Note TN-1446. Port Hueneme, Calif., Jul 1975.

Vesic, A.S. (1970) "Breakout resistance of objects embedded in ocean bottom", in Proceedings of Civil Engineering in the Oceans II, ASCE Conference, Miami Beach, Fla., Dec 10-12, 1969. New York, N.Y., ASCE, 1970, pp 137-165.

Wadsworth, J.F. and Taylor, R.J. (1976) "CEL 10K propellant-actuated anchor", Civil Engineering Laboratory, Technical Note TN-1441. Port Hueneme, Calif., Jun 1976.

Wilson, S.D. and Dietrich, R.J. (1960) "Effect of consolidation pressure on elastic and strength properties of clay", in Proceedings of ASCE Research Conference on Shear Strength of Cohesive Soils, Boulder, Colo., Jun 1960. New York, N.Y., American Society of Civil Engineers.

Zaccor, J.V. and Wallace, M.R. (1963) "Techniques and equipment for determining dynamic properties of soils", Defense Atomic Support Agency. Burlingame, Calif., The United Research Services, 1963. (Contract No. DA-49-146-XZ-019, DASA 1421).

BIBLIOGRAPHY

American Society for Testing Materials (1969). "Vibration effects of earthquakes on soils and foundations," in Proceedings of the Symposium of the Seventy-first Annual Meeting of the American Society for Testing Materials, San Francisco, Calif., Jun 1968. New York, N.Y., 1969. (ASTM Special Technical Publication STP-450)

Baron, W. (1966). The response of cohesive soils to shock loadings, Ph. D. Thesis, Purdue University. Lafayette, Ind., Jun 1966.

Carr, R. W. and Hanna, T. H. (1971). "Sand movement measurement, near anchor plates," Journal of Soil Mechanics and Foundations Division, ASCE, vol 97, no. SM5, May 1971, pp 833-840.

Das, M. B. (1975). "Pullout resistance of vertical anchors," Journal of the Geotechnical Engineering Division, ASCE, vol 101, no. GT1, Jan 1975, pp 87-91.

Hanna, T. H., Sparks, R. and Yilmaz, M. (1972). "Anchor behavior in sand," Journal of the Soil Mechanics and Foundations Division, ASCE, vol 98, no. SM11, Nov 1972, pp 1187-1208. (Proc. Paper 9338)

Healy, K. A. (1971). "Pullout resistance of anchors buried in sand," Journal of the Soil Mechanics and Foundations Division, ASCE, vol 97, no. SM11, Nov 1971, pp 1615-1621. (Proc. Paper 8511)

Kupferman, M. (1971). The vertical holding capacity of marine anchors in clay subjected to static and cyclic loading, M. S. thesis, University of Massachusetts. Amherst, Mass., 1971.

Neely, et al. (1973). "Failure loads of vertical anchor plates in sand," Journal of the Soil Mechanics and Foundations Division, ASCE, vol 99, no. SM9, Sep 1973, pp 669-685. (Proc. Paper 9980)

Seed, H. B., Noorany, I. and Smith, I. M. (1964). Effects of sampling and disturbance on the strength of soft clays, Army Engineers, WES Report no. TE-64-1. Berkeley, Calif., University of California, Department of Civil Engineering, 1964.

Sowers, G. B. and Sowers, G. F. (1970). Introductory soil mechanics and foundations. New York, N.Y., The Macmillan company. 1970.

Vesic, A. S. (1971). "Breakout resistance of objects embedded in ocean bottom," Journal of the Soil mechanics and Foundations Division, ASCE, vol 97, no. SM9, Sep 1971, pp 1183-1205. (Proc. Paper 8372)

Wiegel, R. L. (1964). Oceanographical engineering. Englewood Cliffs, N.J., Prentice-Hall, Inc., 1964.

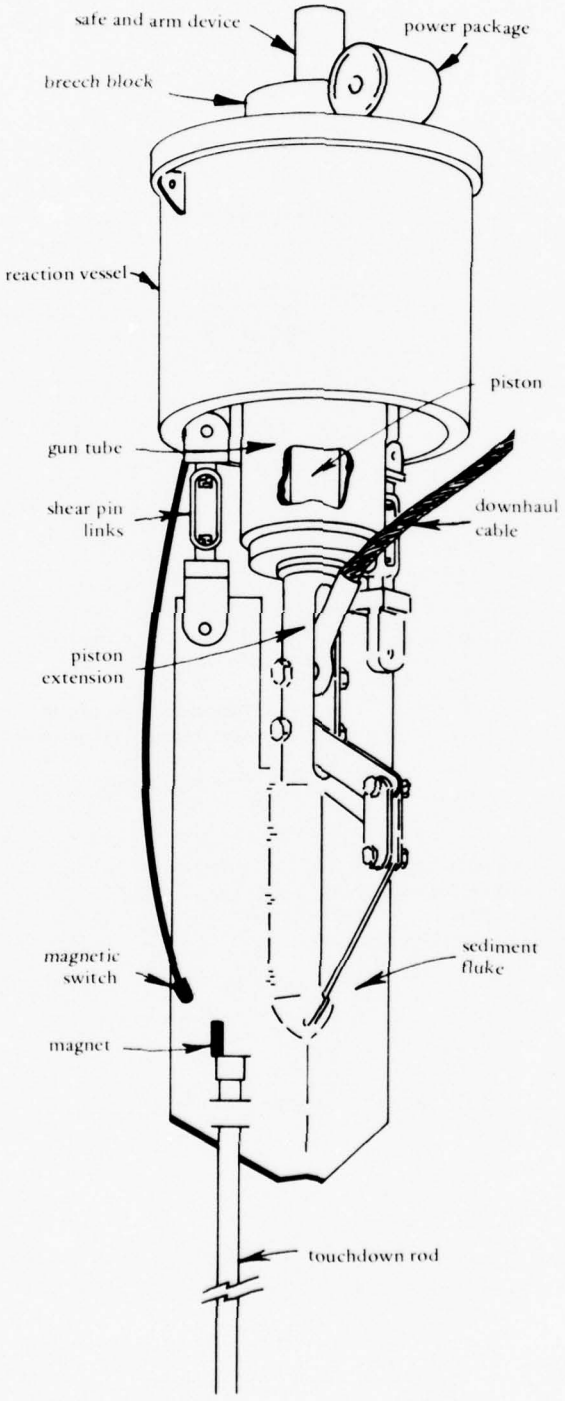

Figure 1. Schematic of CEL 20K propellant anchor (from Taylor, 1976).

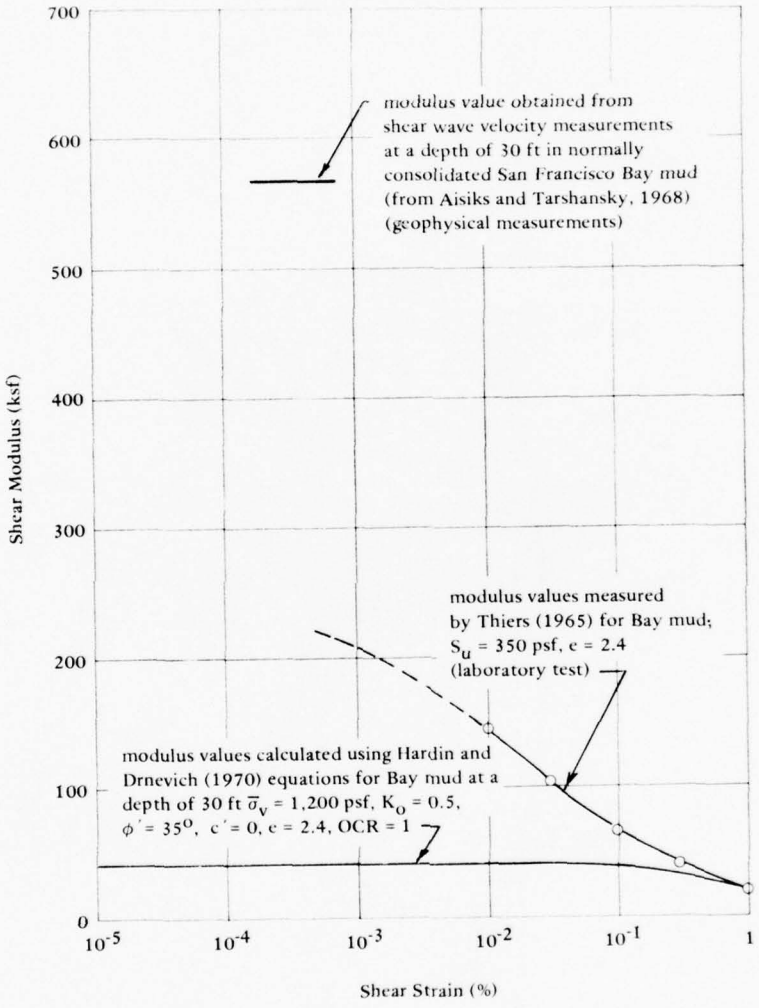

Figure 2. Shear modulus determinations for San Francisco Bay mud (after Seed and Idriss, 1970).

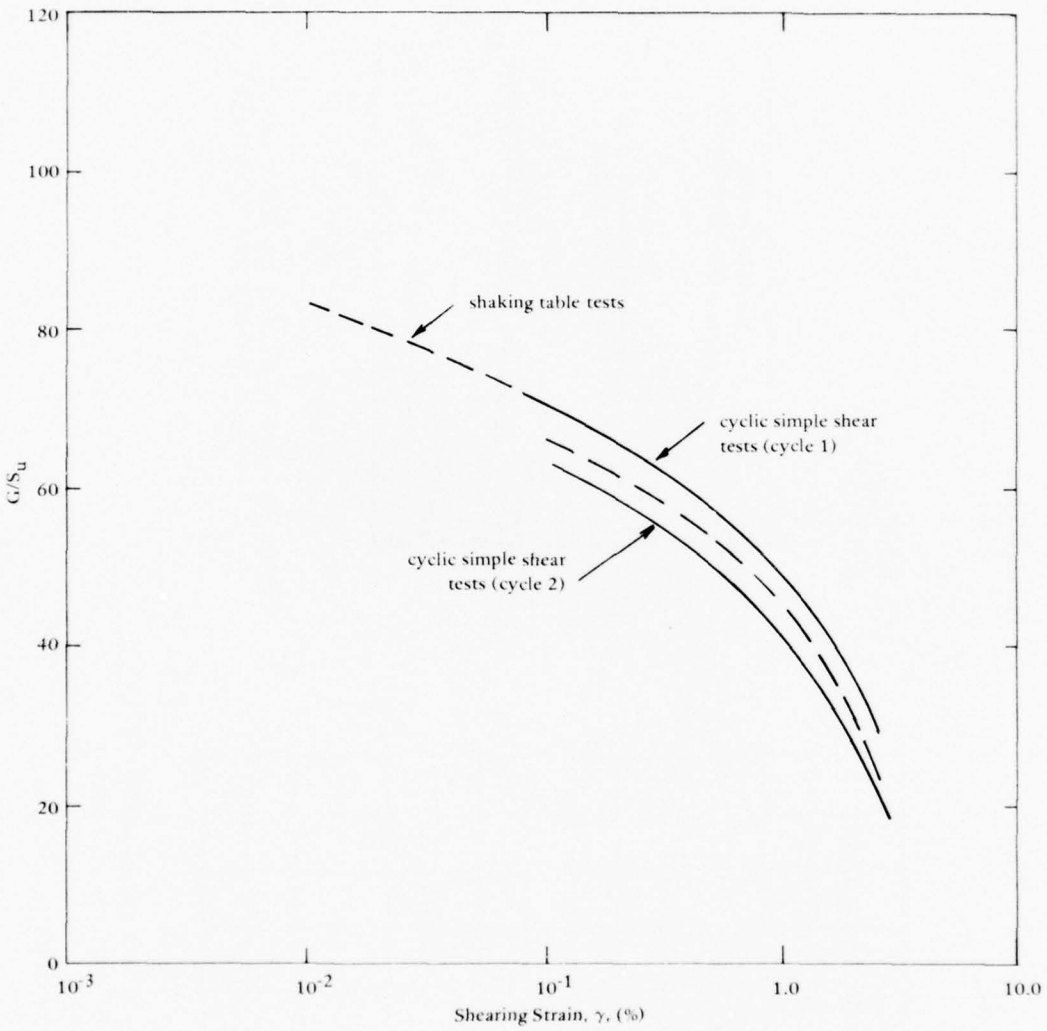

Figure 3. Normalized shear modulus, G/S_u, versus cyclic shear strain for day (from Kovacs et al., 1971).

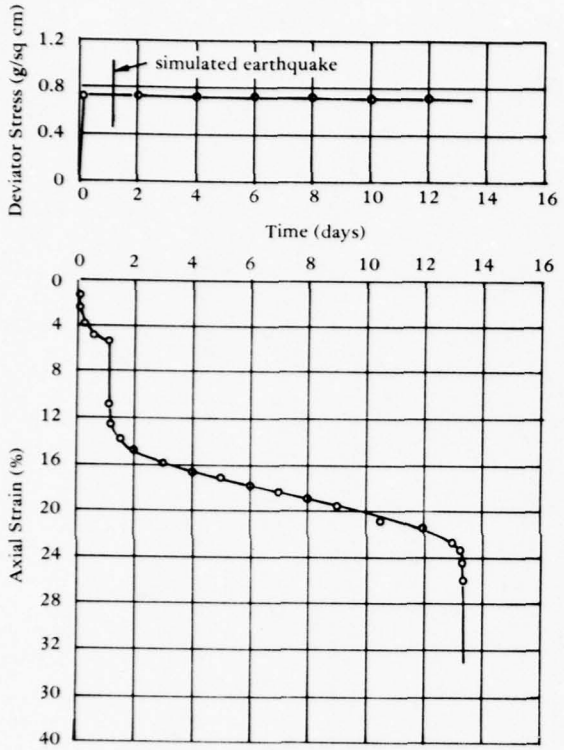

Figure 4. Axial strain increase with time due to simulated earthquake loading on San Francisco Bay mud (from Seed and Chan, 1966).

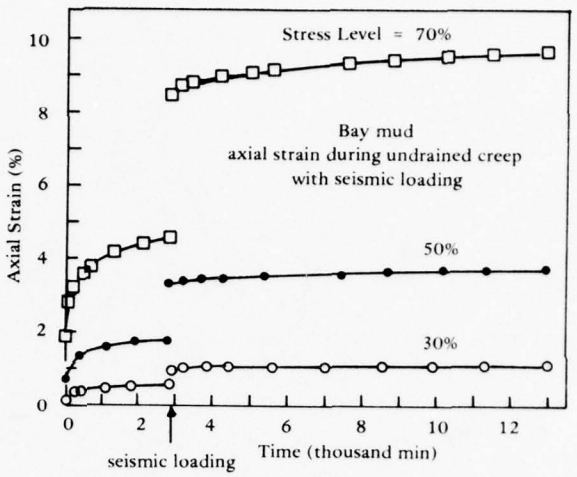

Figure 5. Axial strain as function of time (from Holzer and Hoeg, 1973).

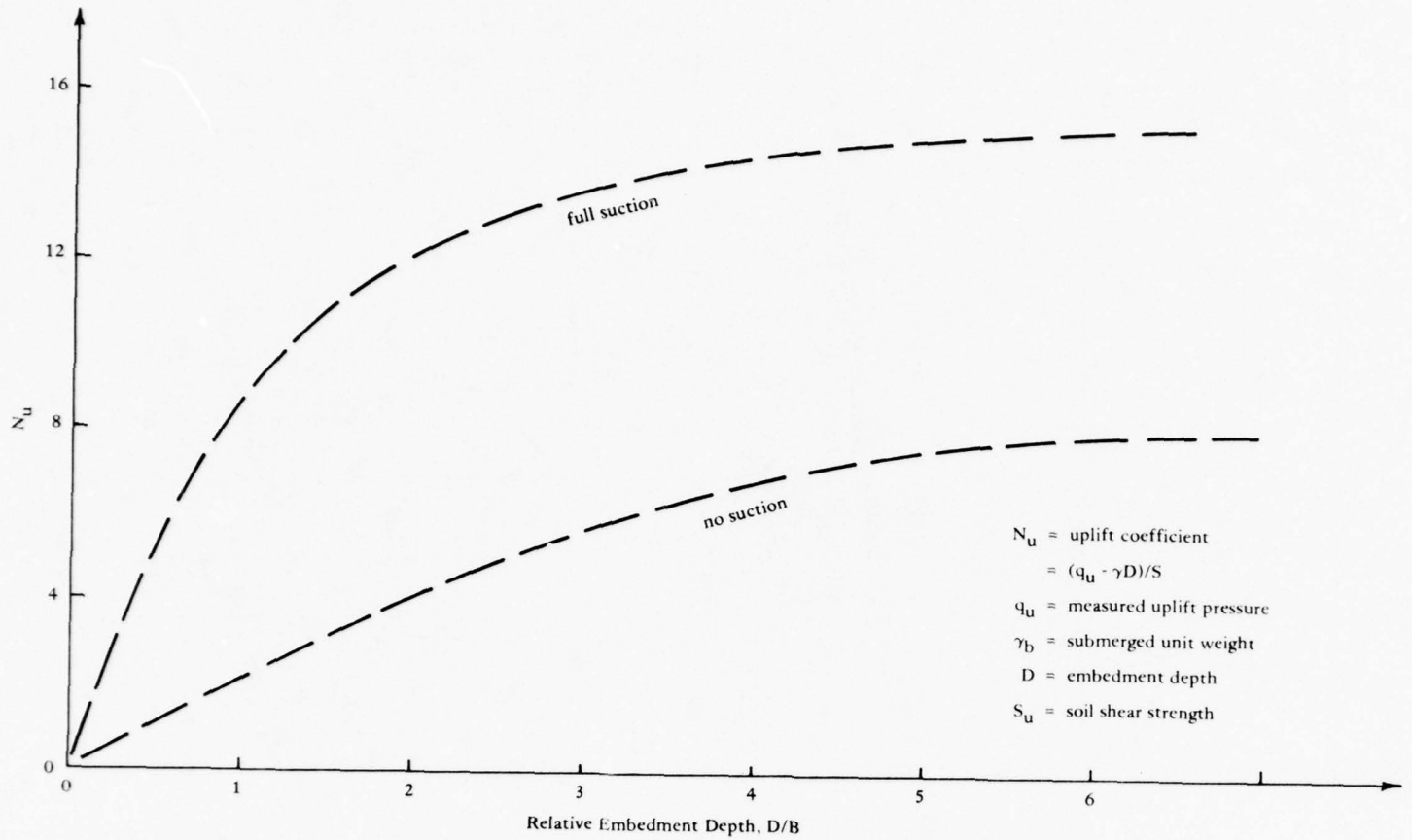

Figure 6. Relationship between uplift coefficient and relative embedment depth, showing the effect of suction on the holding capacity of anchors embedded in clay soil (after Adams and Hayes, 1967).

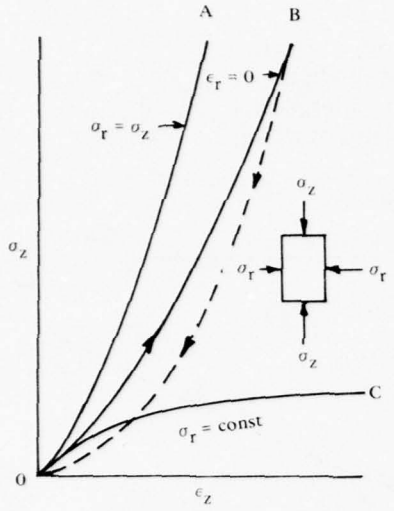

Figure 7. Theoretical stress-strain curves for triaxial tests of granular materials with various lateral restraints (from Richart et. al., 1970).

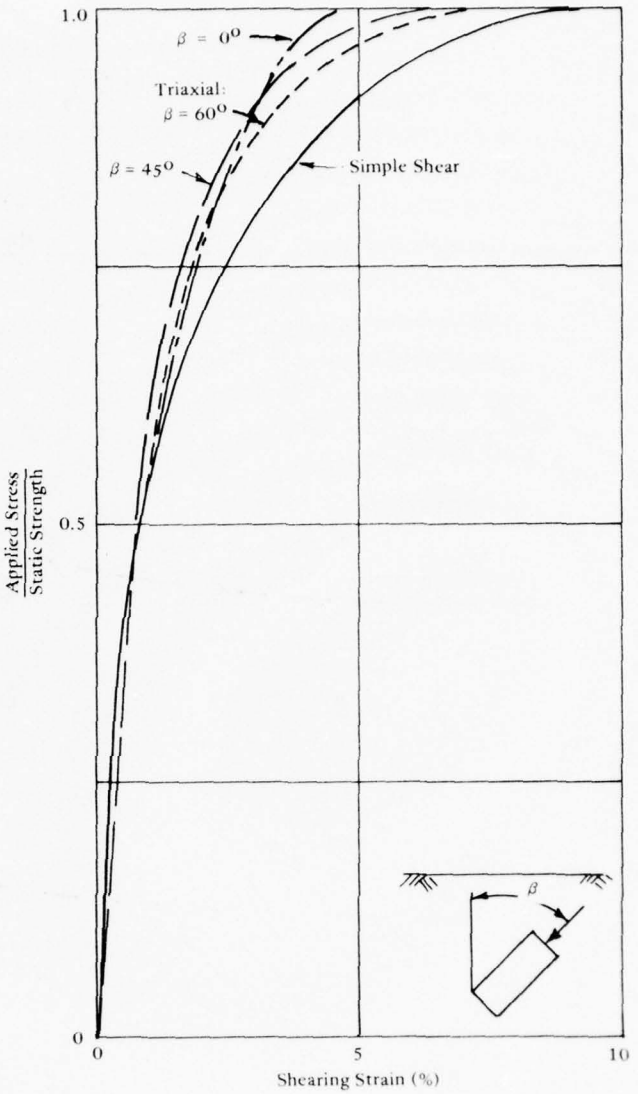

Figure 8. Comparison of normalized stress-strain curves obtained from simple shear and triaxial compression tests (after Thiers and Seed, 1969).

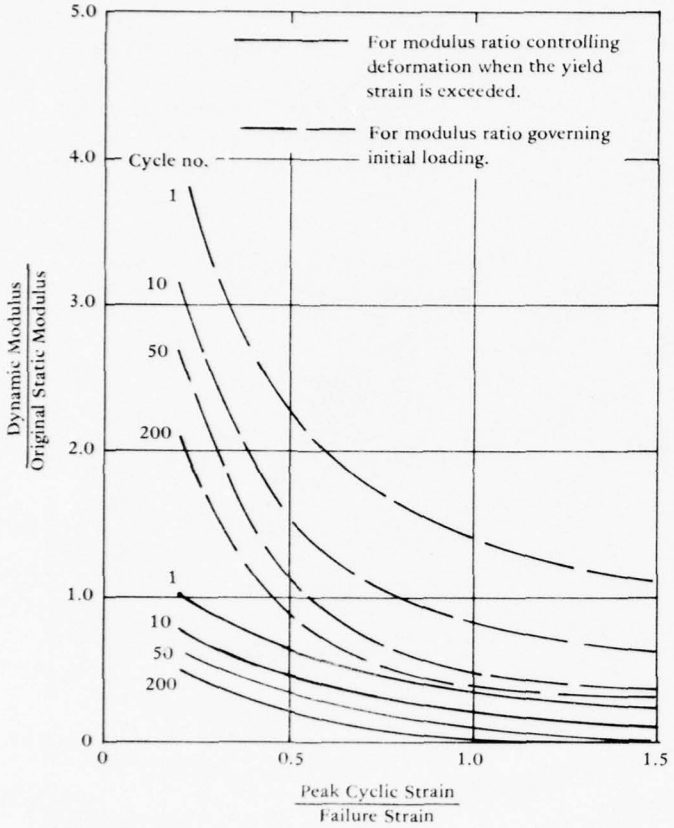

Figure 9. Summary of variation of dynamic modulus ratio with cyclic strain ratio for cycles 1, 10, 50, and 200 (after Thiers and Seed, 1969).

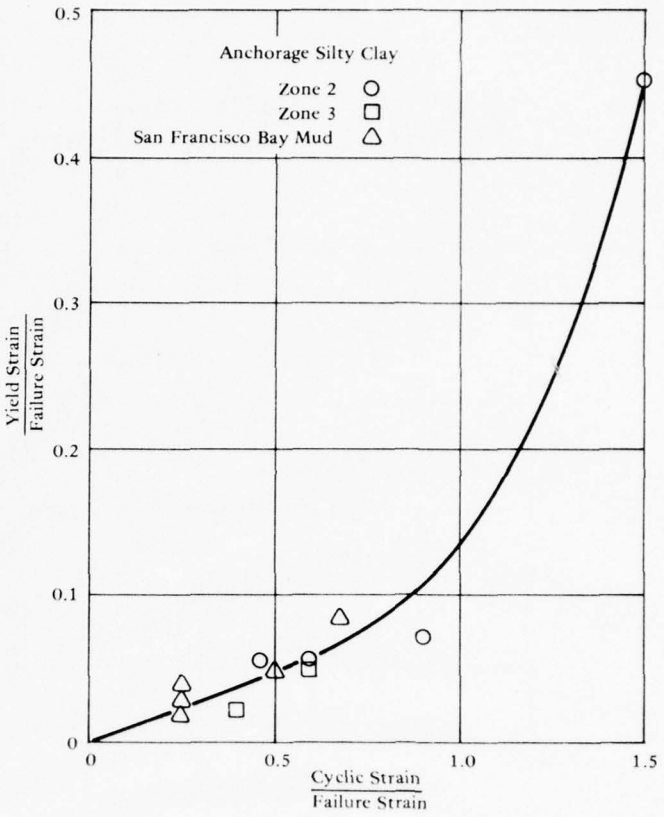

Figure 10. Variation of yield strain ratio with cyclic strain ratio (from Thiers and Seed, 1969).

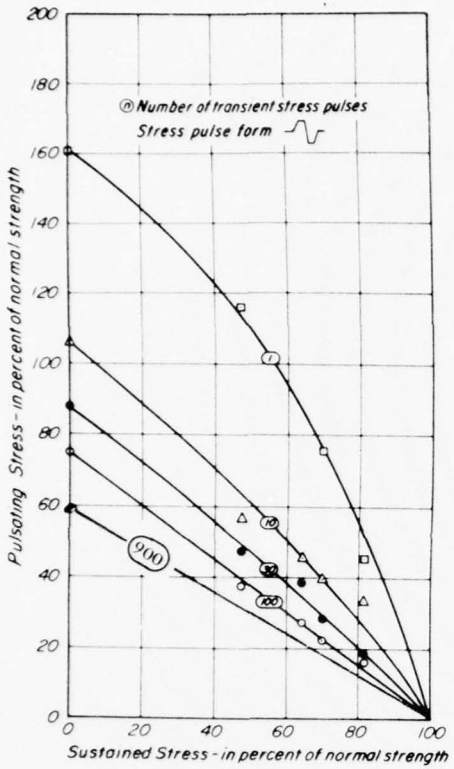

Figure 11. Combinations of sustained and pulsating stress intensities causing failure — San Francisco Bay mud (after Seed and Chan, 1966).

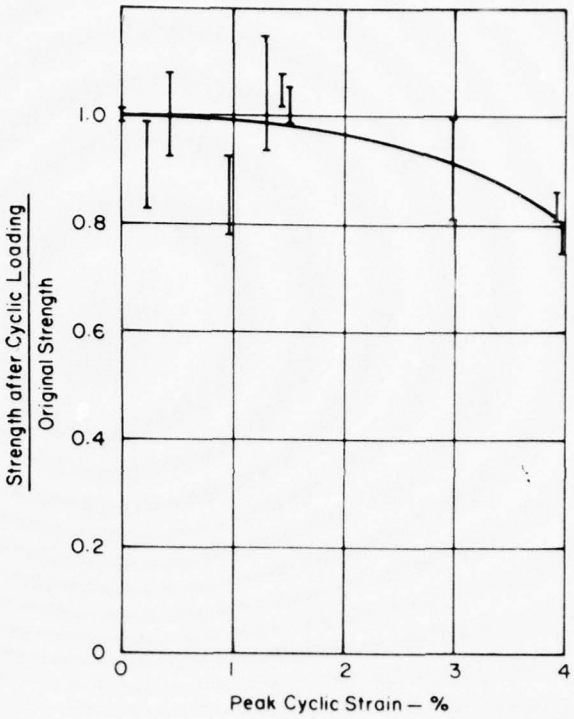

Figure 12. Effect of 200 uniform strain cycles on the strength of clay (from Thiers and Seed, 1969).

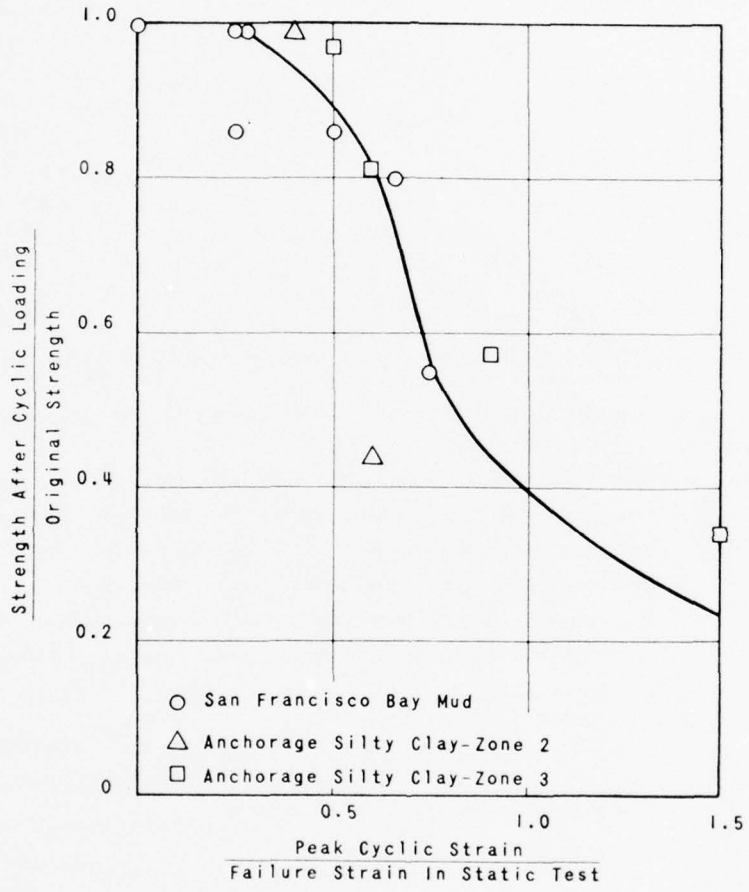

Figure 13. Relationship between normalized strength after cyclic loading versus normalized peak cyclic strain (from Thiers and Seed, 1969).

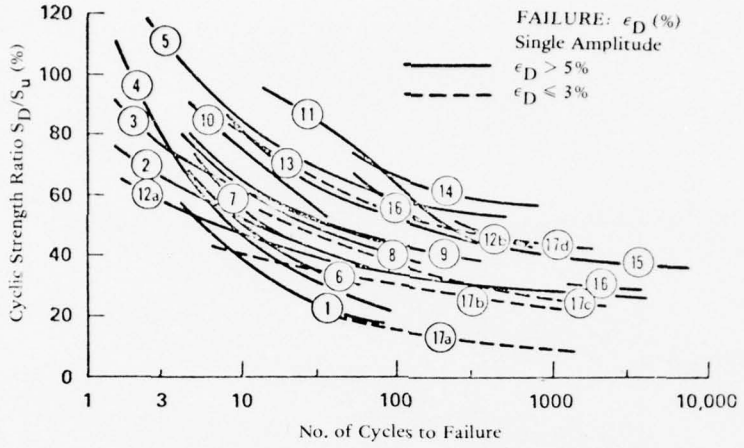

Curve No.	Description
1	Remolded Anchorage Clay, UU (undrained unconfined) Simple Shear, 1 Hz. Thiers and Seed (1969).
2	Undisturbed Hydraulic Fill, Upper San Fernando Dam, CU (confined undrained) Triaxial, 1 Hz.
3	Undisturbed Anchorage Silt, UU Triaxial, 2 Hz. Lee (1964).
4	Compacted Vicksburg Silty Clay, UU Triaxial, 2 Hz. Seed and Chan (1966).
5	Undisturbed San Francisco Bay Mud, UU Triaxial, 2 Hz. Seed and Chan (1966).
6	Undisturbed Anchorage Clay, UU Simple Shear, 1 Hz. Thiers and Seed (1969).
7	Undisturbed San Francisco Bay Mud, UU Triaxial, 1 Hz. Thiers and Seed (1969).
8	Undisturbed San Francisco Bay Mud, UU Simple Shear, 1 Hz. Thiers and Seed (1969).
9	Undisturbed San Francisco Bay Mud, UU Triaxial, Trimmed at 45, 1 Hz. Thiers and Seed (1969).
10	Undisturbed Bootlegger Cove Clay, Anchorage, UU Triaxial, 2 Hz. Seed (1968).
11	Undisturbed Ekofisk Sandy Clay, North Sea, CU Simple Shear (Static strength not well defined).
12	Undisturbed North Sea No. 2; UU Triaxial, 0.5 Hz. (a) Depth 10 to 30 ft below mudline (b) Depth approximately 110 ft below mudline
13	Undisturbed Sedimented Illite, UU Triaxial 0.5 Hz.
14	Gulf of Mexico, UU Triaxial, 0.5 Hz.
15	Undisturbed North Sea No. 2; UU Simple Shear, 0.1 Hz.
16	Model North Sea Clay, Triaxial.
17	Undisturbed North Sea No. 1; CU Triaxial, 0.1 Hz.

Figure 14. Compilation summary of cyclic strength data for saturated clays in symmetrical stress reversing tests (from Lee and Focht, 1975b).

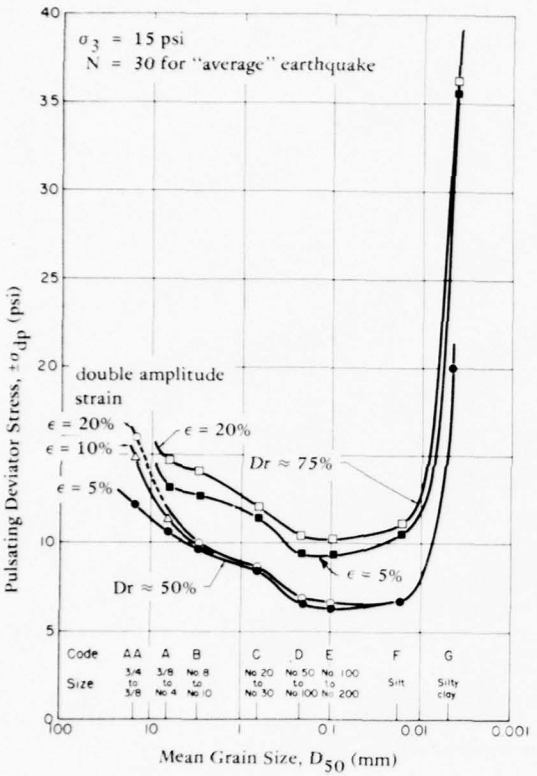

Figure 15. Comparison of pulsating-loading strengths of different grain-sized soils (from Lee and Fitton, 1968).

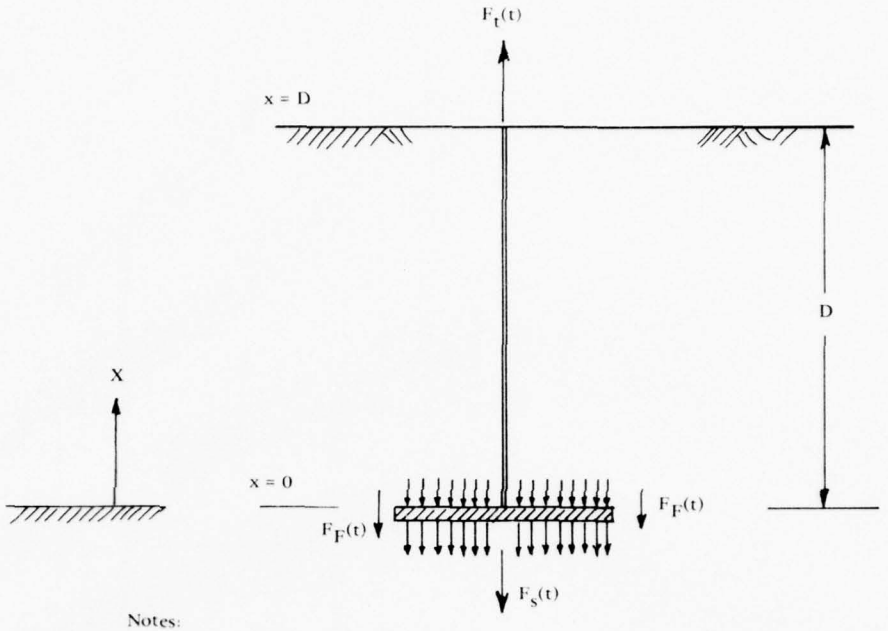

Notes:

X = Rigid body motion of anchor.

x = Distance coordinate along the embedment depth.

$F_t(t)$ = Total uplift force (static + dynamic), w.v.t. time.

$F_s(t)$ = Total suction force along the bottom side of the anchor fluke, w.v.t. time.

$F_F(t)$ = Side frictional force, w.v.t. time.

Figure 16. Forces acting on an embedded anchor being pulled out.

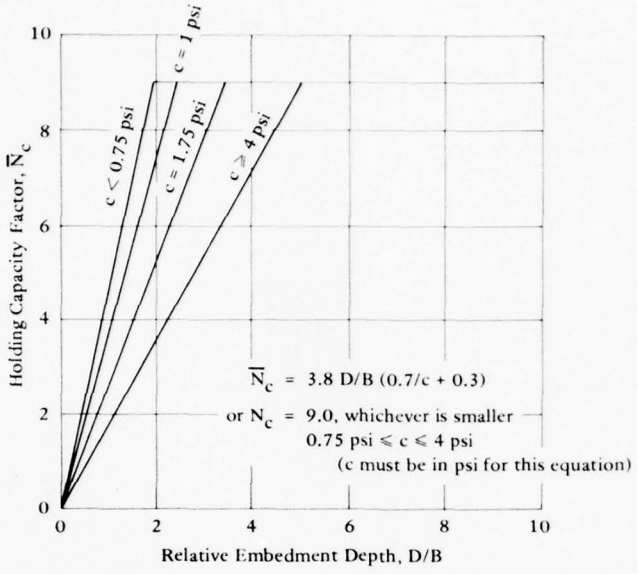

(a) Cohesive soils.

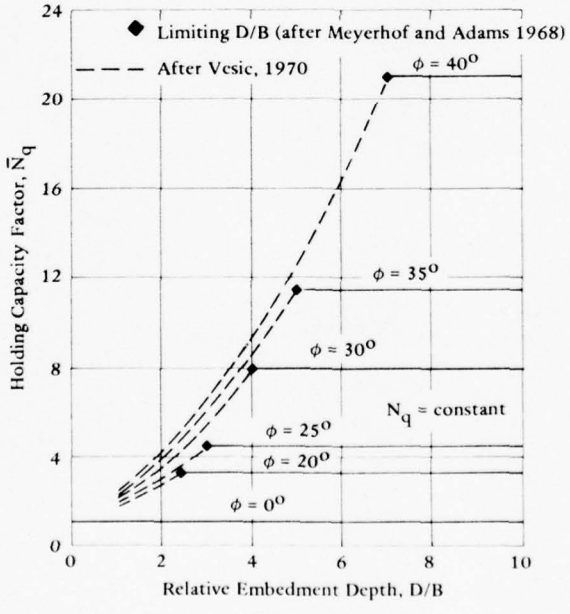

(b) Cohesionless soils.

Figure 17. Relationships between holding capacity factors and the relative embedment depth for various soils (from Taylor and Lee, 1972).

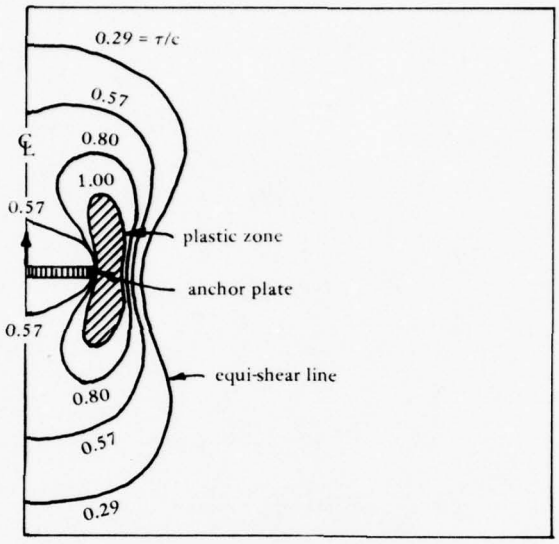

(a) $H_s/AC = 11.9$

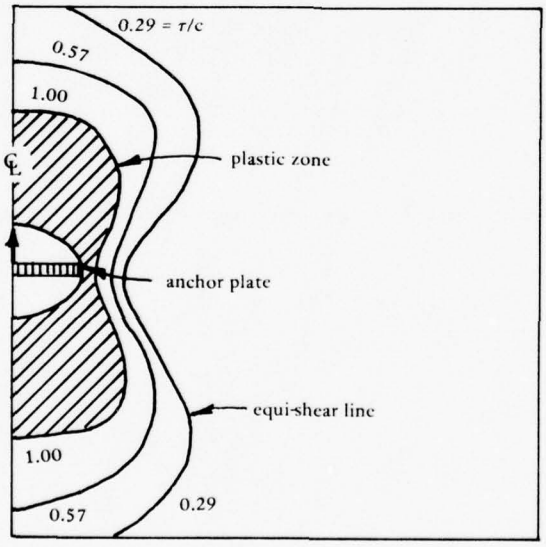

(b) $H_s/AC = 15.9$

Figure 18. Normalized shear stress distributions at normalized loads on a circular anchor plate, with full suction, in an elasto-plastic soil (from Beard, 1974).

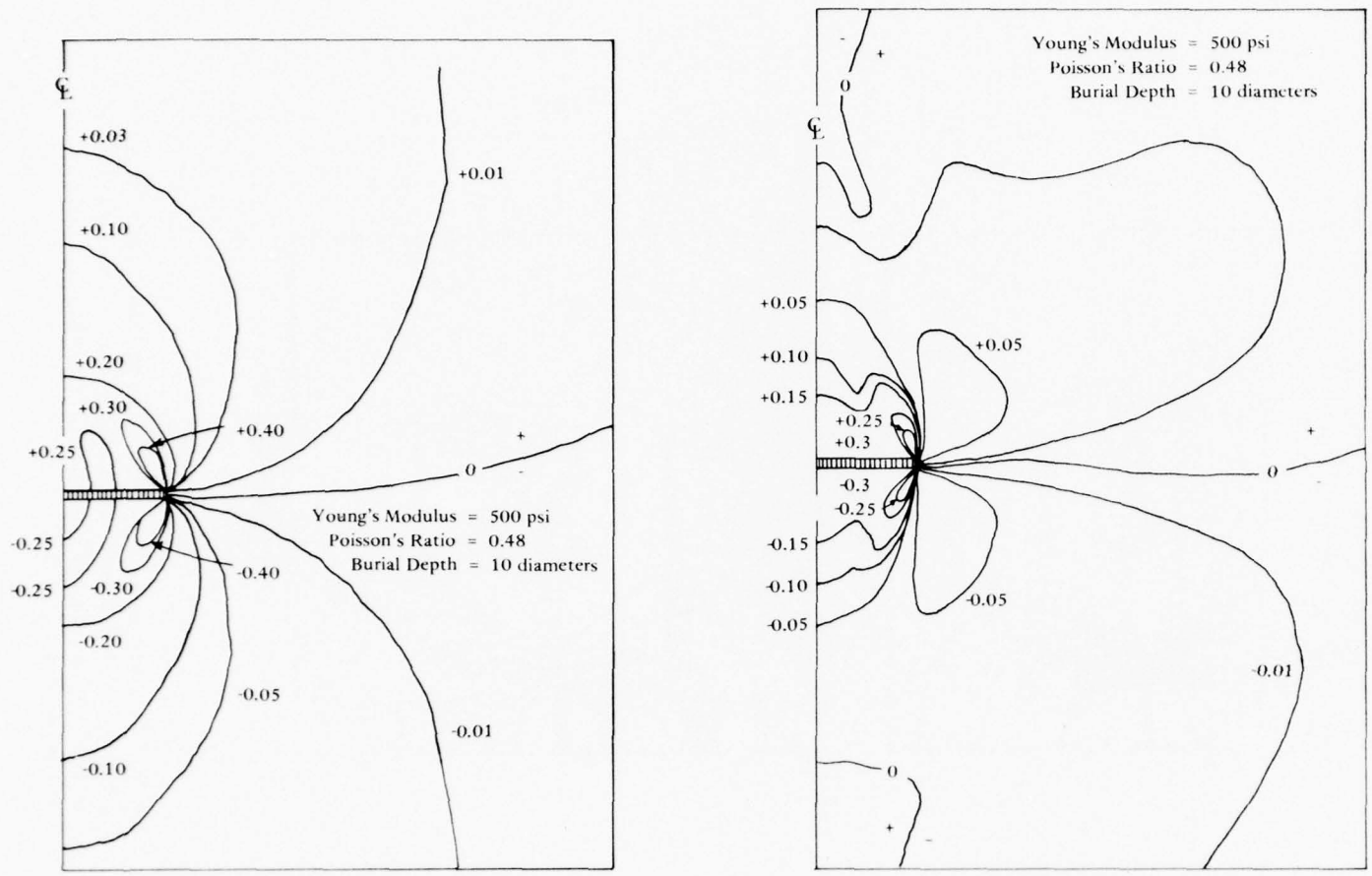

Figure 19. Stresses near an anchor normalized by the average pressure on a circular anchor plate, with full suction, in an elasto-plastic soil (from Beard, 1974).

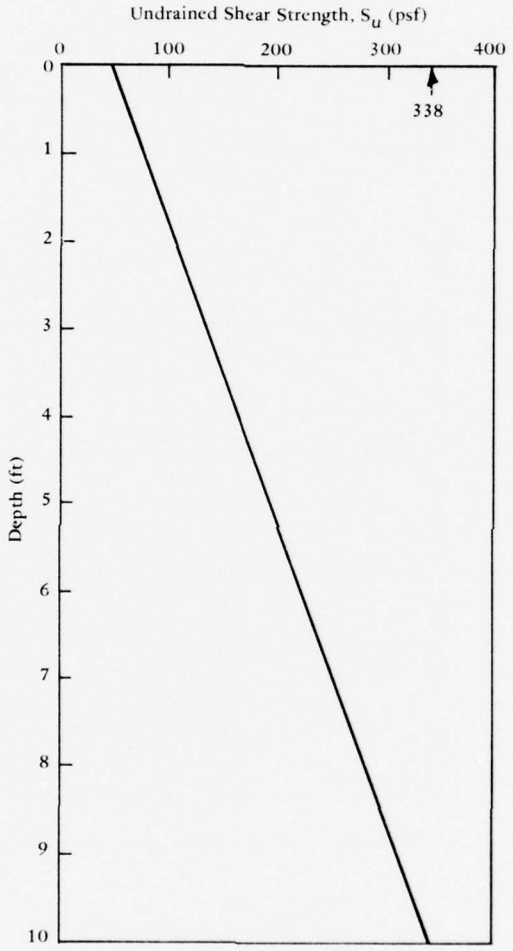

Figure 20. Typical undrained shear strength profile for cohesive seafloor soils (after Lee, 1973).

Table 1. Engineering Properties of Typical Seafloor Soils

Seafloor Soil Type	Site Location	Water Depth (ft)	Sub-bottom Depth (ft)	Atterberg Limits (%)			Average Soil Strength* (psi)	Sensitivity
				Liquid Limit	Plastic Limit	Plasticity Index		
Red Pelagic Clay	1,000 mi north east of Hawaii	18,000	0 - 35	75	35	40	0.3 - 1.0	2-3
Hemipelagic Silty Clay steel gray distal turbidite	Tuft's Abyssal Plain, 1,000 mi. west of Oregon	1,440	0 - 12	50	27	24	0.5 - 3.0	6
Classic nearshore turbidite 10% - 20% foraminifera	Sediment from small basin south east of Puerto Rico	6,000	0 - 5		Nonplastic		1.0 - 3.0 (in place)	2.0 - 2.5
Calcarous ooze with very high foraminifera content (40% - 50%)	Sediment from Blake plateau north of the Bahamas	3,700	0 - 20		Nonplastic		3.0 (in place)	6.0 - 11.0

*Average over the indicated depths of sampling

Table 2. Physical Dimensions and Usage of the CEL Propellant Anchors

Description	CEL 10K Propellant Anchor		CEL 20K Propellant Anchor				CEL 100K Propellant Anchor	
Anchor Assembly:								
Height, (ft)	0		0				14	
Plan Area, (sq ft)	4		4				64	
Total Weight, (lb)	650		2,000				14,000	
Operating Water Depths (ft)								
–Maximum	1,200 (to be extended to 20,000)		20,000				500 (to be extended to 20,000)	
–Minimum	25		50				25	
	Rotating Plate Fluke		Rotating Plate Fluke			Arrowhead-Shaped Projectile	Rotating Plate Fluke	
	Small	Large	Small	Medium	Large		Small	Large
Anchor Projectile:								
Length (ft)	1	2	3	4	5	3	5.5	6.6
Width (ft)	2	2	1.5	2	2.5	0.25	2.75	3.3
Effective Area (sq ft)	2	4	4.5	8	12.5	0.049	13	22
Total Weight (lb)	63	88	300	370	690	275	1,550	1,900
Suitable Seafloor Materials	Sand and Coral	Mud and Clay	Dense Sand and Coral	Sand and Clay	Mud and Soft Clay	Rock and Hard Coral	Sand and Coral	Mud and Clay
Penetration Depth (ft)	5 to 25	25 to 35	5 to 20	20 to 30	30 to 40	2 to 5	7 to 30	30 to 50
Holding Capacity (lb)	20,000	10,000	50,000	30,000	20,000	70,000	200,000	100,000

Table 3. Nature of Dynamic Loads Affecting Embedment Anchors

Load Source	Loading Period[a]	Magnitude Ratio of Dynamic (Peak-to-Peak) Component to Static Component	
		Possible Range	Likely Value in Deep Ocean Submerged Mooring
Loads in Line[b] caused by:			
-- Current -- Fluctuations	1 Hour to 1 Year	Up to 1	0.05
-- Waves	2 to 20 Seconds	Up to 1	0.005
-- Vortex Shedding	0.5 to 1 Second	0.005 to 0.05	0.01
-- Impact or Line Snap	0.01 to 1 Seconds	Up to 5	0.2
-- Earthquakes	0.1 to 2 Seconds	Up to 0.1	0.05
-- Underwater Blasts	0.01 to 0.1 Seconds	Up to 0.2	0.01
Loads in Sediment caused by:[c]			
-- Earthquakes	0.1 to 2 Seconds	Up to .5	0.1
-- Underwater Blasts	0.01 to 0.1 Seconds	Up to 5	0.01

a The effective period of a one-time step loading is taken as five times the rise time.
b Static component is anchor working load.
c Static component is soil stress under anchor working load.

Appendix A

LOADS FROM VORTEX SHEDDING (CABLE STRUMMING)

A constant static buoyant load from a buoy is assumed on the upper end of the cable. An oscillating force in the cable applied to the buoy will create oscillatory motions having an insignificant amplitude for the frequencies of concern. Hence, the initial length and the span of the cable may be assumed to be equal. For a sagging cable, these assumptions also are valid in the biaxial curvilinear coordinate system having axes along and perpendicular to the static cable axis.

For a cable of initial length and fixed span L, the stretched length in the deflected shape of n/2 full sine wave cycles having an amplitude a is

$$S_n = L\left[1 + \frac{1}{4}\left(\frac{n\,\pi\,a}{L}\right)^2\right] \qquad \text{(A-1)}$$

The strain is

$$\varepsilon_s = \frac{S_n - L}{L} = \frac{1}{4}\left(\frac{n\,\pi\,a}{L}\right)^2 \qquad \text{(A-2)}$$

Cable strumming occurs when the excitation frequency corresponds to the resonant frequency of the cable in water. The excitation frequency is

$$f_s = \frac{V}{5\,D_c} \qquad \text{(A-3)}$$

where V = current velocity

D_c = cable diameter

The resonant frequency is

$$f_n = \frac{n}{2\,L}\left(\frac{T}{m}\right)^{1/2} \qquad \text{(A-4)}$$

where T = cable tension

m = cable mass per unit length

Equating the two frequency expressions (Equations A-3 and A-4) and solving for n gives

$$n = 2L \frac{V}{5 D_c} \left(\frac{m^{1/2}}{T^{1/2}} \right) \tag{A-5}$$

Substituting this expression for n into Equation A-2 gives

$$\varepsilon_s = \frac{1}{4} \left(\frac{\pi a}{L} \right)^2 \left[2L \frac{V}{5 D_c} \left(\frac{m^{1/2}}{T^{1/2}} \right) \right]^2$$

$$= \frac{\pi^2 a^2}{4 L^2} \left(\frac{4 L^2 V^2 m}{25 D_c^2 T} \right)$$

or

$$\varepsilon_s = \frac{\pi^2 a^2}{4 (25)} \left(\frac{4 m}{\pi D_c^2} \right) \left(\frac{V^2 \pi}{T} \right) \tag{A-6}$$

but the volumetric equivalent for the mass per unit length is

$$m = \rho \frac{\pi D_c^2}{4} \tag{A-7}$$

where ρ = cable mass per unit volume

Solving Equation A-7 for ρ and combining the result with Equation A-6 gives

$$\varepsilon_s = \left(\frac{V a \pi}{10} \right)^2 \frac{\rho \pi}{T} \tag{A-8}$$

The dynamic load increment is the product of the elastic modulus, the cable area, and the strain increment caused by strumming:

$$\Delta T = E \frac{\pi D_c^2}{4} \varepsilon_s \tag{A-9}$$

Substituting equation A-8 into Equation A-9 and dividing by T gives the relative dynamic load increment as:

$$\frac{\Delta T}{T} = \frac{E \pi D_c^2}{4} \left(\frac{V a \pi}{10T}\right)^2 \rho \pi \qquad \text{(A-10a)}$$

or

$$\frac{\Delta T}{T} = E A_c \left(\frac{V a \pi}{10T}\right)^2 \rho \pi \qquad \text{(A-10b)}$$

Example calculations are presented in Table A-1 to illustrate relative values of the dynamic load increment for a typical deepwater mooring. As shown, the dynamic load increment is about 2% of the static load for a current 2 knots, and nearly 5% for a current of 3 knots. As the number of cycles during a 10-year life span in a 2-knot current is about 2.2×10^9, the effect of this type of dynamic loading on anchor holding capacity is potentially significant. Soil test data are needed at these low levels of load and high numbers of cycles to enable predictions to be made of these effects.

Table A-1. Example Values of Relative Dynamic Load Increment for a Strumming Cable

Current Velocity, V		Relative Dynamic Load Increment $\Delta T/T$	Frequency, $f_s \approx \frac{V}{5D_c}$
(ft/s)	(knots)		(Hz)
0.5	0.30	0.00046	1
1.0	0.59	0.00185	2
1.5	0.89	0.0042	3
2.0	1.18	0.0074	4
2.5	1.48	0.0116	5
3.0	1.78	0.0166	6
3.5	2.07	0.0227	7
4.0	2.37	0.0296	8
4.5	2.66	0.0375	9
5.0	2.96	0.0463	10

Notes: (1) 1 knot = 1.689 ft/s

(2) $$\frac{\Delta T}{T} = E A_c \left(\frac{V a \pi}{10T}\right)^2 \rho \pi$$

where T (cable tension) = 20,000 lb

ρ (cable mass per unit volume) = 15 lb-s^2/ft^4

A_c (cable cross-sectional area) = $\pi D^2/4$ = 0.007854 ft^2

a (strumming amplitude) = D_c (cable diameter) = 0.1 ft

E (cable tensile elastic modulus) = 200×10^7 lb/ft^2

Then

$$\frac{\Delta T}{T} = \left(\frac{V}{23.2 \text{ ft/s}}\right)^2$$

$$f_s = \left(\frac{V}{0.5 \text{ ft/s}}\right)$$

or

$$\frac{\Delta T}{T} = \left(\frac{V}{13.8 \text{ knots}}\right)^2$$

$$f_s = \left(\frac{V}{0.296 \text{ knots}}\right)$$

Appendix B

RADIATION DAMPING AND STIFFNESS

In a lumped system the dashpot usually represents the damping of the soil. Two types of damping are usually considered. One is caused by the loss of energy through stress wave propagation throughout the surrounding soil in a soil-mass system (in our case an soil-anchor system); this damping is commonly known as "radiation damping". The other type of damping is associated with internal energy losses within the soil due to hysteretic and viscous effects. Usually the internal damping is neglected because it is small relative to the radiation damping.

By definition the damping ratio (D_R) is the ratio of the damping value to the critical damping value.

$$D_R = \frac{c'}{c_c} \qquad \text{(B-1)}$$

where $c_c = 2\sqrt{km}$

c' = damping constant

k = stiffness constant

m = mass constant

Hardin and Drnevich (1972) derived expressions for the soil's elastic response at a given strain as follows. A *reference strain*, was defined in terms of the plasticity index (P.I.), the effective vertical stress, and the overconsolidation ratio as shown in Figure B-1. Next, a *hyperbolic strain* was defined in terms of the reference strain and the given soil strain level of concern, as shown in Figure B-2. Then, a maximum value of shear modulus was expressed as

$$G_{max} = \frac{1230\ (2.973 - e)^2}{(1 + e)}\ (OCR)\ K\ \bar{\sigma}_o^{1/2} \qquad \text{(B-2)}$$

in which e = void ratio

OCR = overconsolidation ratio

$\bar{\sigma}_o$ = mean principal effective stress (Kg/cm^2)

K = coefficient of lateral stress which depends on the plasticity index as shown in Table B-1.

(Alternatively, G_{max} may be evaluated by seismic testing on laboratory vibration testing).

Similary, a maximum value of damping ratio was expressed for saturated cohesive soils as

$$D_{R_{max}} = 31 - (3 + 0.03\ f)\ \bar{\sigma}_o^{1/2} + 1.5 f^{1/2} - 1.5\ (\log n) \quad \text{(B-3)}$$

where f = frequency, cycles/s.

Finally, ratios between the values of D_R and G of concern and their corresponding maxima were expressed in terms of the hyperbolic strain as shown in Figure B-3.

The following example illustrates the use of this method.

Problem: It is desired to determine the values of modulus and damping for the tenth cycle of loading at a depth of 20 feet in a saturated silty clay layer of soil. Pertinent conditions are:

f = 1 cps

e (at 20 ft) = 0.95

P.I. = 32%

$\bar{\sigma}_v$ = effective stress = 9 psi (at 20 ft)

γ = shear strain of soil = 0.1%

$= 10 \times 10^{-4}$

soil is normally consolidated

Solution: From Figure B-1 for P.I. = 32% and e = 0.95

$$\frac{\gamma_r}{\sqrt{\bar{\sigma}_o}} = 1.2 \times 10^{-4} = 0.00012$$

The value of the effective stress corresponding to a depth of 20 feet is 9 psi. Hence, the reference strain can be obtained:

$$\frac{\gamma_r}{\sqrt{9}} = 1.2 \times 10^{-4}$$

or

$$\gamma_r = 3.6 \times 10^{-4} \text{ in./in.}$$

Dividing the shear strain value of the soil (γ) by the reference strain (γ_r) gives the following strain ratio

$$\gamma/\gamma_r = (10 \times 10^{-4})/(3.6 \times 10^{-4}) = 2.8$$

For these values of effective stress and strain ratio, Figure B-2 gives the hyperbolic strain (γ_h) for damping as being equal to 2.9. Then from Figure B-3, the following values are obtained:

$$\frac{G}{G_{max}} = 0.26 \text{ and } \frac{D_R}{D_{R_{max}}} = 0.74$$

From Equations B-2 and B-3, the corresponding maxima are

$$G_{max} = 6{,}800 \text{ psi}$$

and

$$D_{R_{max}} = 29\%$$

Then the required value of the shear modulus is

$$G = 0.26\ (G_{max})$$

$$= 0.26 \times 6{,}800 = 1{,}770 \text{ psi}$$

and the required value of the damping ratio is

$$D_R = 0.74\ (D_{R_{max}})$$

$$= 0.74 \times 0.29 = 0.2149 = 21.5\%$$

The value of the damping ratio is usually in the range of 4% to 23% (Hardin and Drnevich, 1972), depending on the type of soil encountered, for a shear strain amplitude of less than 0.1%. For seafloor soils under increased strain levels, somewhat higher values of damping ratio would be appropriate.

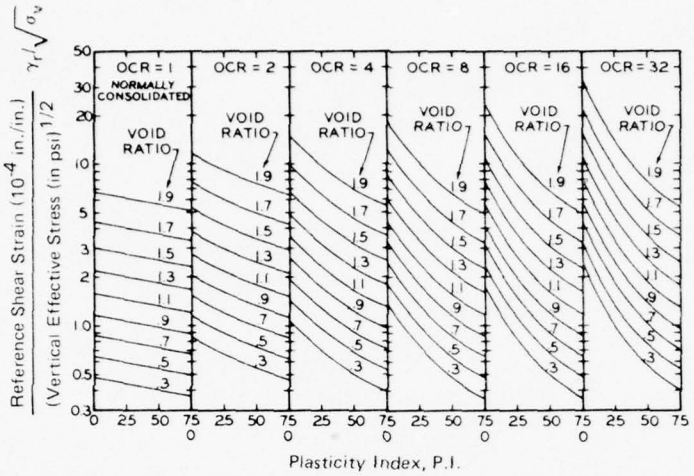

Figure B-1. Relationship between the ratio of the reference shear strain and the vertical effective stress versus the plasticity index for cohesive soils (from Hardin and Drnevich, 1972).

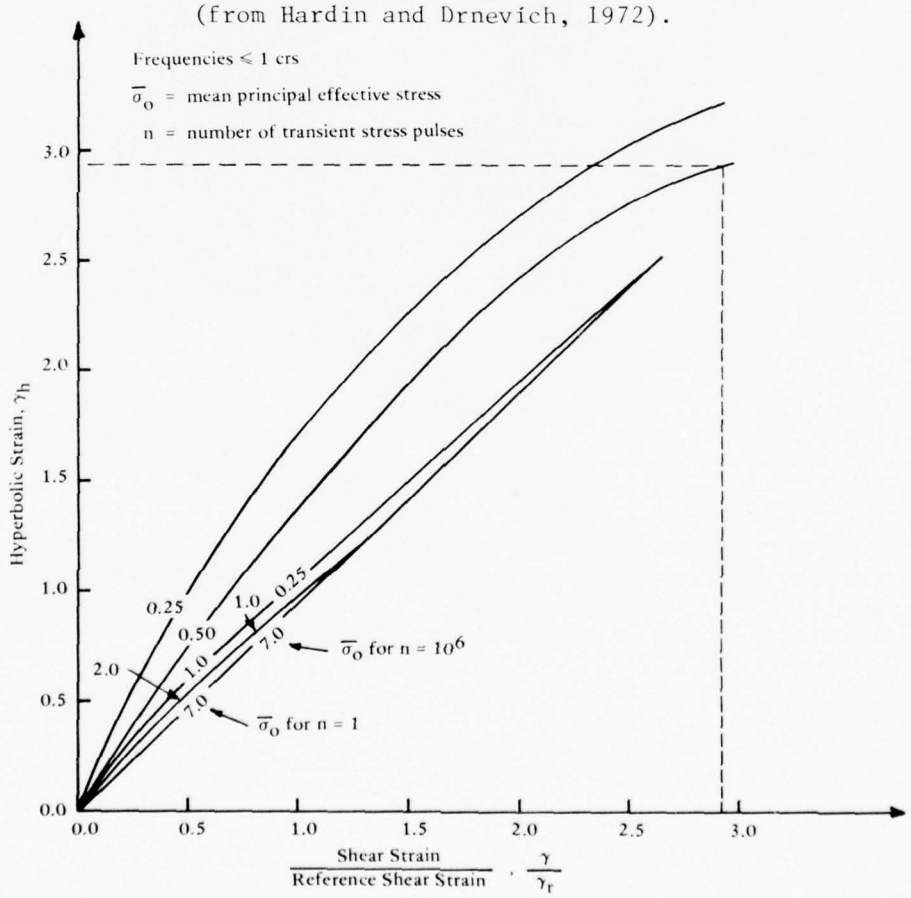

Figure B-2. Hyperbolic strain versus normalized shear strain for damping in saturated cohesive soils (after Hardin and Drnevich, 1972).

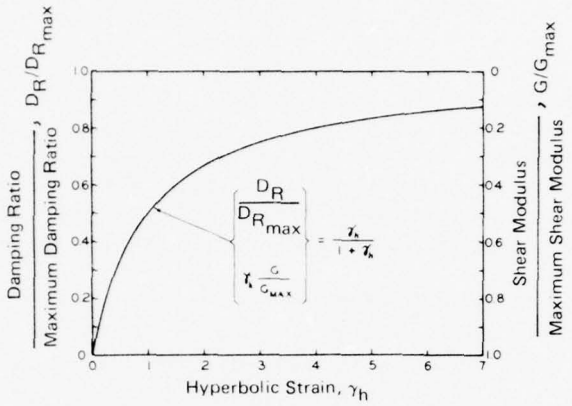

Figure B-3. Relationship between normalized shear modulus and damping ratio for all soil versus hyperbolic strain (from Hardin and Drnevich, 1972).

Table B-1. Values for Coefficient of Lateral Stress and Plasticity Index

Plasticity Index (P.I.)	Coefficient of Lateral Stress, (K)
0	0
20	0.18
40	0.30
60	0.41
80	0.48
100	0.50

Appendix C

DYNAMIC LOAD MAGNIFICATION

When a system consisting of an anchor, a seafloor soil, an anchor cable, and an anchored object is loaded dynamically, its response may be amplified if the loading frequency is near a resonant frequency of either the system or a portion of the system. This "dynamic load magnification" may be evaluated by using textbook methods directly for some modes of load application and by augmenting these methods with judgment for others.

Such a method is presented here for the vertical excitation of an embedded anchor plate that is used to moor an object subjected to vertical loading from waves, with the anchor line experiencing cable strumming. Figure C-1 shows values of the magnification factor M_a for surface footings for various values of the mass ratio B_z plotted against the dimensionless frequency a_o. In order to use this figure for embedded plates, the applied load and the mass of the anchored system should each be cut in half, so that the resulting half-space representation will correspond to the idealization used as a basis for the figure. With this adjustment, the resulting predictions do not require adjustment.

Typical relevant parameters are given in Table C-1 for small, medium, and large anchors. The loads from waves and strumming are considered separately, and corresponding approximations are given for the effective vertically oscillating masses (including water-added mass, for the wave loading). As shown, values of B_z range from 0.08 to 20, and values of dimensionless loading frequency range from 0.003 to 0.09. The responses at resonance are shown in Figure C-2, with predictions of magnification factor at resonance M_m extended to high values of B_z by the indicated formulas. It is apparent that considerable magnification might be expected for conditions approaching resonance. However, for the relatively low-frequency cases given in Table C-1, Figure C-1 shows that values of M_a are essentially unity.

Although these values are representative of common anchor applications, it is possible that loadings would be nearer to resonance and hence higher magnifications would occur for rapidly loaded, high-mass systems in weak, low-modulus soils. Hence, each specific case should be considered carefully to determine if a value of M_a greater than unity should be applied to loading magnitudes.

Transient loadings are not covered directly by the above analysis. A step load having a rapid rise time can produce dynamic overshoot, up to twice that resulting from a quasi-static application of the same level of load. In cases where the rise time of a step loading may be short, a magnification factor of two may be applied conservatively.

Impactive loadings are most easily analyzed by determining the kinetic energy imparted to the system during the impact and then determining the system response as that required for the energy to be absorbed during a quasi-static movement of the system. (The absorbed energy is equal to the area under a quasi-static load-displacement diagram.) If an anchor is to sustain only a few impact loads, considerable nonrecoverable upward movement may be acceptable for energy absorption. However, if many impacts are anticipated, the anchor should be designed to absorb the energy within the elastic range of movement in order to prevent eventual pullout.

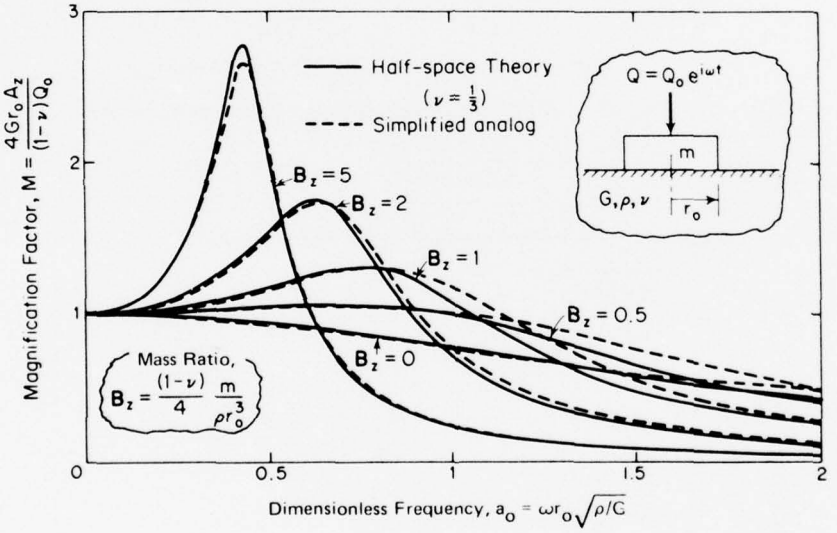

Figure C-1. Response of rigid circular footing to vertical force developed by constant force excitation (after Lysmer, et al., 1966).

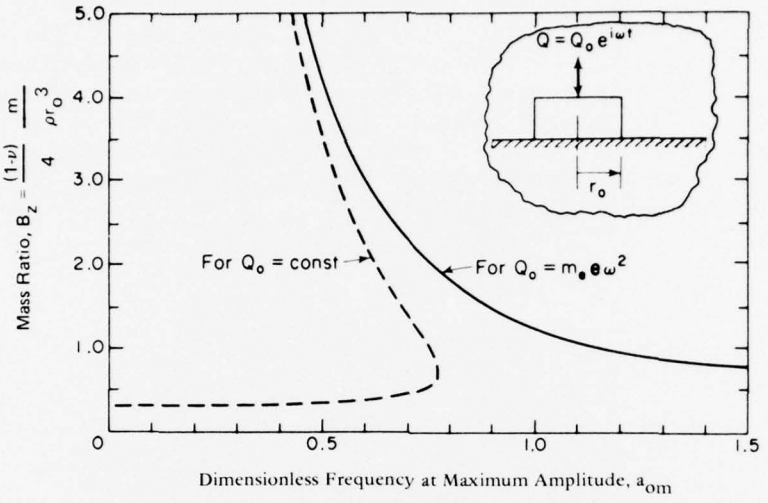

(a) Mass ratio versus dimensionless frequency at resonance.

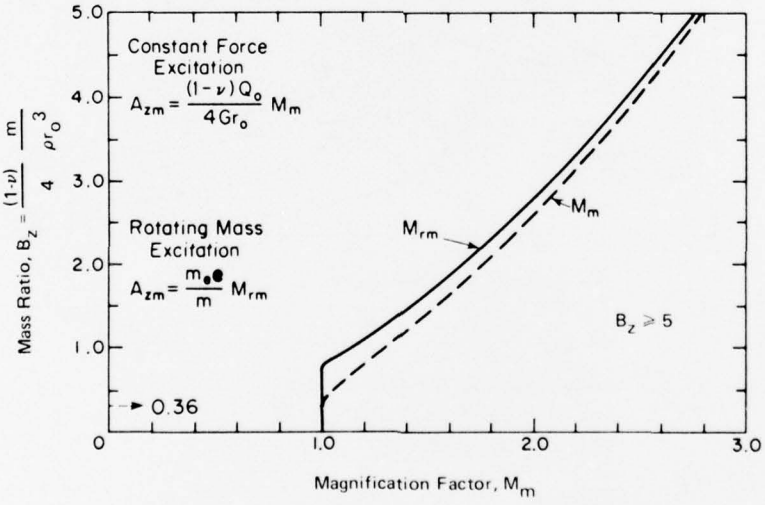

(b) Mass ratio versus magnification factor at resonance.

Figure C-2. Vertical oscillation of rigid circular footing on elastic half-space (after Richart, et al., 1970).

Table C-1. Typical Relevant Parameters for Anchor, Soil, and Anchored Object Idealized as Cyclically Loaded Single-Degree-of-Freedom System

Typical Loading Source	Mooring Elements	Anchor's Effective Circular Plate Radius r_o (ft)	Total Effective Mooring Weight $m_e g$ (lb)	Mass Ratio B_z [a]	Loading Frequency f (Hz)	Dimensionless Loading Frequency a_o [b]
Waves	anchor, soil, line, object	1	31,600	20.4	0.4	0.0044
		1.732	100,000	12.5	0.2	0.0037
		3	316,000	7.6	0.1	0.0033
Cable Strumming	anchor, soil, 500 ft of line	1	316	0.204	8	0.087
		1.732	1,000	0.125	4	0.074
		3	3,160	0.076	2	0.065

Notes:

a $B_z = C_B \frac{(1 - \nu)}{4} \frac{m_e}{\rho r_o^3}$, where $\nu = 0.5$ $\rho g = 96.6$ lb/ft^3, $g = 32.2$ ft/sec^2, $C_B =$ 1/2 for deeply embedded plate

b $a_o = \omega r_o \sqrt{\frac{\rho}{G}}$, where $\omega = 2 \pi f$, $G = 1{,}000{,}000$ lb/ft^2

Appendix D

HYSTERETIC DAMPING

The magnification effects described above reflect damping arising mainly from the geometrical dispersion of energy at low strains. When strains are high, falling in the range of 0.1% to 1%, energy losses in the soil should increase damping significantly, thus reducing magnification factor values, particularly at or near resonance.

Energy losses may be estimated from the areas enclosed by the hysteresis loops described on the stress-strain diagrams for the soil elements surrounding an anchor. In order to do this without any prior knowledge of anchor response, the soil element strains must be known, and the element energy losses must be integrated to yield an estimate of total energy loss per cycle of loading. Such a procedure will be carried out during the mathematical modeling phase of current research. As an alternative, the hysteresis loop for the anchor load-displacement diagram may be used, if it can be estimated from field or model test data.

The effective damping factor for a surface plate, when no hysteresis energy losses occur in the soil, is given by Richart et al., (1970) in their Equation 7-30 as

$$c_z = 0.425 \frac{c_c}{\sqrt{B_z}} \qquad \text{(D-1)}$$

where c_c = critical damping constant

B_z = mass ratio

In this expression, the critical damping constant is

$$c_c = 2\sqrt{m\, k_z} \qquad \text{(D-2)}$$

where m = mass of lumped oscillating elements

k_z = idealized single-degree-of-freedom stiffness

The stiffness is evaluated for a surface plate as

$$k_z = \frac{4\, G\, r_o}{(1 - \nu)} \qquad \text{(D-3)}$$

The mass ratio is evaluated as

$$B_z = \frac{(1 - \nu)}{4} \frac{m}{\rho r_o^3} \tag{D-4}$$

These relationships may be used directly for a deeply embedded anchor plate where the soil below the depth of the plate plays no part in mobilizing pullout resistance, and also may be used for an embedded plate where suction is operative beneath the plate if the plate load and plate mass are halved. Thus,

$$c_c = \sqrt{2 m_e k_z} \tag{D-5}$$

and

$$B_z = \frac{(1 - \nu)}{8} \frac{m_e}{\rho r_o^3} \tag{D-6}$$

where m_e = total effective oscillating mass for a single-degree-of-freedom idealization of an embedded anchor plate, with suction operative.

The energy loss to damping in one cycle in a single-degree-of-freedom system is given by

$$E_c = c' \pi \omega z_p^2 \tag{D-7}$$

where c' = effective damping constant

ω = circular frequency

z_p = peak displacement amplitude

If this energy loss is equated to the area enclosed by the load-displacement hysteresis loop, defined as E_h, the result can be rearranged and evaluated to determine an effective damping as

$$c_h = \frac{E_h}{\pi \omega z_p^2} \tag{D-8}$$

It can be demonstrated that the effective damping associated with static hysteresis losses (Equation D-8) may be substantially greater than that associated with geometrical dispersion (Equation D-1) and that the total effective damping ($c_z + c_h$) may range from less than 5% to more than 100% of critical (Equation D-2), depending upon the anchor mass loading and displacement levels.

The dynamic load magnification curves given in Appendix C are for insignificant hysteresis effects. As discussed by Richart et al. (1970), the magnification is reduced to values less than unity, at any loading frequency, when the total effective damping constant is increased beyond 0.707; significant reductions also result from values somewhat less than 0.707.

An iterative procedure that may be noted to account for damping during resonance in the manner discussed above is as follows. B_z is calculated from Equation D-6, and the relationship given in Figure C-2 is used to determine M_m. An amplitude A_{zm} is determined from the static load-displacement curve at a load equal to the product of the specified static load Q_o with the magnification factor M_m; then the energy dissipation per cycle E_h is determined from the area enclosed by the hysteresis loop. The effective hysteretic damping factor c_h is then calculated from Equation D-8.

The mass ratio corresponding to no hysteretic damping B_z is calculated from Equation D-4, and the corresponding geometrical damping factor c_z is calculated from Equation D-1. The total damping factor c_c is calculated as the sum of c_z and c_h, and a new effective mass ratio B_e is calculated from an inverted form of Equation D-1.

B_e is then substituted for B_z in the relationships given in Figure C-2 to determine a new magnification factor M_m and a new amplitude A_{zm}. The new values are used to repeat the process: a new E_h, a new c_h, a new c_e, and a new B_e are obtained, leading to still another M_m and A_{zm}, and these steps are repeated until a desired precision is indicated by a close agreement between the old and new values of M_m. The peak load is obtained as the product of Q_o with M_m.

LIST OF SYMBOLS

A	Cross-sectional area (L^2)
A_c	Cable cross-sectional area (L^2)
A_f	Anchor fluke plan area (L^2)
A_z	Amplitude of vertical vibration (L)
A_{zm}	Amplitude from static load displacement curve (L)
a	Strumming amplitude (L)
a_o	Dimensionless frequency (cycles/s)
B	Anchor fluke diameter or width (L)
B_e	Effective mass ratio
B_z	Mass ratio for vertical vibration of rigid circular footing on elastic half-space
C_B	Constant for half-embedded foundation
c	Unit soil cohesion (F/L^2)
c'	Effective damping constant (FT/L)
$\bar{c}$	Cohesion intercept based on effective stress (F/L^2)
c_c	Critical damping constant (FT/L)
c_h	Damping constant from hysteresis loop (FT/L)
c_z	Damping constant for vertical vibration (FT/L)
D	Anchor fluke embedment depth (L)
D_c	Diameter of anchor cable (L)
D_R	Damping ratio
$D_{R_{max}}$	Maximum damping ratio
D_r	Relative density of cohesionless soils
D_{so}	Particle size diameter at which 50% of the soil is finer (L)
D/B	Relative embedment depth

E	Cable tensile elastic modulus (F/L^2)
E_c	Energy loss to damping
E_h	Energy loss from hysteresis loop
e	Voids ratio, also base of natural logarithm
E_f	Side frictional force with respect to time (F)
F_r	Soil dynamic resistance force (F)
F_s	Total suction force along the bottom side of the anchor fluke, with respect to time (F)
F_t	Total uplift force (static plus dynamic), with respect to time (F)
f	Frequency (cycles/s)
f_n	Resonant frequency (cycles/s)
f_s	Excitation frequency (cycles/s)
G	Soil shear modulus (F/L^2)
G_{max}	Maximum soil shear modulus (F/L^2)
H_s	Static holding capacity (F)
H_T	Total holding capacity (static plus dynamic) (F)
i	$\sqrt{-1}$
K	Coefficient of lateral stress
K_o	Coefficient of lateral stress at rest
k	Stiffness
k_z	Idealized single-degree-of-freedom stiffness
L	Anchor fluke length (L)
L_c	Anchor cable length (L)
M	Total mass of anchor plus cable plus oscillating soil (FT^2/L)
M_a	Amplitude magnification factor
M_m	Magnification factor

m	Mass constant
m_e	Total effective oscillating mass
N	Number for average earthquake
$\bar{N}_c$, $\bar{N}_q$	Holding capacity factors
N_u	Uplift coefficient
n	Number of transient stress pulses
OCR	Overconsolidation ratio
Q	Time-dependent external force acting on elastic system (F)
Q_o	Amplitude of external force acting on elastic system (F)
q_u	measured uplift pressure (F/L^2)
r_o	Radius of circular footing on circular anchor fluke (L)
S_n	Stretched length in the deflected shape of a full sine wave cycle (L)
S_D	Cyclic shear strength (F/L^2)
S_u	Static undrained shear strength (F/L^2)
T	Cable tension (F)
t	Time (T)
V	Velocity of water current (F/T)
X	Rigid body motion of anchor
x	Distance coordinate along the embedment depth
$\ddot{a}$	Measured acceleration (L/T^2)
z_p	Peak displacement amplitude (L)
β	Angle between vertical and axial applied stress in triaxial test
γ	Shear strain of sort
γ_b	Buoyant unit weight (F/L^3)
γ_h	Hyperbolic strain

γ_r	Reference strain
ε	Double amplitude strain
ε_D	Cyclic strain amplitude (L)
ε_r	Normal strain in r direction
ε_s	Strain in cable due to strumming effect
ε_z	Normal strain in the z direction
ν	Poisson's ratio
π	Numerical constant (3.14159)
ρ	Mass per unit volume (FT^2/L^4)
σ_3	Confining pressure (F/L^2)
σ_{dp}	Pulsating deviator stress (F/L^2)
σ_r	Radial normal stress (F/L^2)
σ_z	Vertical normal stress (F/L^2)
$\bar{\sigma}_o$	Mean principle effective stress (F/L^2)
$\bar{\sigma}_v$	Vertical effective stress (F/L^2)
τ	Shearing stress (F/L^2)
τ/c	Normalized shear stress
ϕ	Angle of internal friction in cohesionless soils
ϕ'	Effective angle of internal friction in cohesionless soils
ω	Circular frequency (rad/s)

DISTRIBUTION LIST

AFB AFCEC/XR, Tyndall FL; CESCH, Wright-Patterson; SAMSO/DEB, Norton AFB CA; Stinfo Library, Offutt NE
ARMY BMDSC-RE (H. McClellan) Huntsville AL; DAEN-MCE-D Washington DC; Tech. Ref. Div., Fort Huachuca, AZ
ARMY BALLISTIC RSCH LABS AMXBR-XA-LB, Aberdeen Proving Ground MD
ARMY COASTAL ENGR RSCH CEN Fort Belvoir VA; R. Jachowski, Fort Belvoir VA
ARMY CONSTR ENGR RSCH LAB Library, Champaign IL
ARMY CORPS OF ENGINEERS MRD-Eng. Div., Omaha NE; Seattle Dist. Library, Seattle WA
ARMY CRREL A. Kovacs, Hanover NH
ARMY ENG DIV HNDED-CS, Huntsville AL
ARMY ENG WATERWAYS EXP STA Library, Vicksburg MS
ARMY ENGR DIST, Library, Portland OR
ARMY ENVIRON. HYGIENE AGCY Water Qual Div (Doner), Aberdeen Prov Ground, MD
ARMY MATERIALS & MECHANICS RESEARCH CENTER Dr. Lenoe, Watertown MA
ARMY MOBIL EQUIP R&D COM Mr. Cevasco, Fort Belvoir MD
ASST SECRETARY OF THE NAVY Spec. Assist Energy (P. Waterman), Washington DC; Spec. Assist Submarines, Washington DC
BUREAU OF RECLAMATION Code 1512 (C. Selander) Denver CO; MC 1541 (J. P. Bara), Denver CO
MCB ENS S.D. Keisling, Quantico VA
CNO Code NOP-964, Washington DC; Code OPNAV 90H; OP987P4 (B. Petrie), Pentagon
COMSUBDEVGRUONE Operations Offr, San Diego, CA
DEFENSE DOCUMENTATION CTR Alexandria, VA
DEFENSE INTELLIGENCE AGENCY Dir., Washington DC
DNA STTL, Washington DC
DOD Explosives Safety Board (Library), Washington DC
DTNSRDC Code 1548 (T. Tsai), Bethesda MD
ENERGY R&D ADMIN. Dr. Cohen
HQFORTRPS 2nd FSCG, (Caudillo) Camp Lejeune, NC
MARINE CORPS BASE Code 43-260, Camp Lejeune NC; M & R Division, Camp Lejeune NC; PWO, Camp S. D. Butler, Kawasaki Japan
MARINE CORPS DIST 9, Code 043, Overland Park KS
MARINE CORPS HQS Code LFF-2, Washington DC
MCAS Code PWE, Kaneohe Bay HI; Code S4, Quantica VA; PWO Kaneohe Bay HI
MCRD PWO, San Diego Ca
MCSC B520, Barstow CA
MILITARY SEALIFT COMMAND Washington DC
NAS SCE, Barbers Point HI
NAVCOMMSTA PWO, Adak AK
NAVFACENGCOM Code 2014 (Mr. Taam), Pearl Harbor HI
NAVPGSCOL Code 61WL (O. Wilson); E. Thornton, Monterey CA
NAVSCOLCECOFF C35; C44A (R. Chittenden), Port Hueneme CA
NAVSECGRUACT PWO, Torri Sta, Okinawa
NAVSHIPREPFAC Library, Guam
NAVSHIPYD Code 410, Mare Is., Vallejo CA; Commander, Vallejo, CA; PWO, Mare Is.
NAVSTA PWO Midway Island; SCE, Subic Bay, R.P.
NAVSUPPACT CO, Seattle WA
NAD Code 011B-1, Hawthorne NV; Engr. Dir. Hawthorne, NV
NAF PWO Sigonella Sicily
NAS Lead. Chief. Petty Offr. PW/Self Help Div, Beeville TX; PWD Maint. Div., New Orleans, Belle Chasse LA; PWO Key West FL; PWO Belle Chasse, LA; PWO Chase Field Beeville, TX; PWO, Miramar, San Diego CA; SCE Lant Fleet Norfolk, VA
NATPARACHUTETESTRAN PW Engr, El Centro CA
NAVPHIBASE UCT 1 (Hall) Norfolk, VA
NAVAL FACILITY PWO, Brawdy Wales UK; PWO, Cape Hatteras, Buxton NC; PWO, Centerville Bch, Ferndale CA
NAVCOASTSYSLAB Code 423 (D. Good), Panama City FL; Code 710.5 (J. Mittleman) Panama City, FL; Code 710.5 (J. Quirk) Panama City, FL; Library Panama City, FL

NAVFACENGCOM Code 0433B Alexandria, VA; Code 0451 Alexandria, VA; Code 04B3 Alexandria, VA; Code 04B5 Alexandria, VA; Code 101 Alexandria, VA; PC-22 (E. Spencer) Alexandria, VA; PL-2 Ponce P.R. Alexandria, VA
NAVFACENGCOM - CHES DIV. Code 101 Wash, DC; Code 403 (H. DeVoe) Wash, DC; Code FPO-1 (Ottsen) Wash, DC; Code FPO-1C2 Wash, DC; Code FPO-1T3 (Mr. Scola), Washington DC
NAVFACENGCOM - LANT DIV. RDT&ELO 09P2, Norfolk VA
NAVFACENGCOM - NORTH DIV. (Boretsky); Code 1028, RDT&ELO, Philadelphia PA; ROICC, Contracts, Crane IN
NAVFACENGCOM - PAC DIV. Code 402, RDT&E, Pearl Harbor HI; Commander, Pearl Harbor, HI
NAVFACENGCOM - SOUTH DIV. Code 90, RDT&ELO, Charleston SC; Dir., New Orleans LA
NAVFACENGCOM - WEST DIV. AROICC, Point Mugu CA; Codes 09PA; O9P/20
NAVHOSP LT R. Elsbernd, Puerto Rico
NAVOCEANO Code 1600 Wash, DC; Code 3412 (J. Kravitz) Wash, DC
NAVPHIBASE Code S3T, Norfolk VA; OIC, UCT 1 Norfolk, VA
NAVSHIPYD Code 440, Norfolk; PWO Portsmouth, NH
NAVSTA CO Roosevelt Roads P.R.; CO Mayport FL; Engr. Dir., Rota Spain; Maint. Div. Dir/Code 531, Rodman Canal Zone; PWD/Engr. Div, Puerto Rico; PWO, Keflavik Iceland; PWO, Puerto Rico; ROICC, Rota Spain
NAVSURFWPNCEN PWO, White Oak, Silver Spring, MD
NAVWPNCEN PWO (Code 70), China Lake CA
NAVWPNENGSUPPACT Code ESA-733, Washington DC
NAVWPNSTA PWO Yorktown, VA
NAS CO, Guantanamo Bay Cuba; Code 114, Alameda CA; Code 183, Dir Engr Div., San Diego, CA; Code 18700, Brunswick ME; OIC, CBU 417, Oak Harbor WA; PWD (ENS E.S. Agonoy), Chase Field, Beeville TX; PWD, Maintenance Control Dir., Bermuda; PWO (M. Elliott), Los Alamitos CA
NATL OCEAN AND ATMDS. ADMIN. Libraries Div.-D823, Silver Spring MD
NATL RESEARCH COUNCIL Naval Studies Board, Washington DC
NAVACT PWO, London UK
NAVCOASTSYSLAB CO, Panama City FL
NAVCOMMSTA PWO Kenitra Morocco; PWO, Norfolk VA
NAVCONSTRACEN CO (CDR C.L. Neugent), Port Hueneme, CA
NAVELEXSYSCOM Code PME-124-61, Washington DC
NAVFACENGCOM CDR L K Donovan, Alexandria VA; Code 0453 (D. Potter) Alexandria, VA
NAVFACENGCOM - CHES DIV. Code 402 (R. Morony) Wash, DC; Code FPO-1 (C. Bodey) Wash, DC; Code FPO-1SP (Dr. Lewis) Wash, DC; Code FPO-1SP13 (T F Sullivan) Wash, DC
NAVFACENGCOM - NORTH DIV. Code 09P (LCDR A.J. Stewart); Design Div. (R. Masino), Philadelphia PA
NAVFACENGCOM - WEST DIV. Code 04B
NAVFACENGCOM CONTRACTS Bethesda, Design Div. (R. Lowe) Alexandria VA; Eng Div dir, Southwest Pac, Manila, PI; OICC/ROICC, Balboa Canal Zone; ROICC, Diego Garcia Island; TRIDENT (CDR J.R. Jacobsen), Bremerton WA 98310
NAVMARCORESTRANCEN ORU 1118 (Cdr D.R. Lawson), Denver CO
NAVOCEANSYSCEN CODE 4099 (E. Hamilton), San Diego CA; Code 409 (D. G. Moore), San Diego CA; Code 6344 (R. Jones); Code 65 (H. Talkington); Code 6565 (Tech. Lib.), San Diego CA; Code 7511 (PWO)
NAVPETOFF Code 30, Alexandria VA
NAVPGSCOL D. Leipper, Monterey CA
NAVSCOLCECOFF CO, Code C44A
NAVSEASYSCOM Code SEA OOC Washington, DC
NAVSEC Code 6034 (Library), Washington DC
NAVSHIPYD Code 202.4, Long Beach CA; Code 440 Portsmouth NH; L.D. Vivian; PWD (LT N.B. Hall), Long Beach CA
NAVSTA SCE, Guam; Utilities Engr Off. (LTJG A.S. Ritchie), Rota Spain
NAVSUPPACT AROICC (LT R.G. Hocker), Naples Italy
NAVWPNCEN ROICC (Code 702), China Lake CA
NAVWPNSTA ENS G.A. Lowry, Fallbrook CA
NAVWPNSUPPCEN PWO Crane IN
NAVXDIVINGU LT A.M. Parisi, Panama City FL
NAVEDTRAPRODEVCEN Tech. Library
NAVFACENGCOM - LANT DIV. Eur. BR Deputy Dir, Naples Italy
NAVSUBASE LTJG D.W. Peck, Groton, CT
NCBC CEL (CAPT N. W. Petersen), Port Hueneme, CA; CEL AOIC; Code 10 Davisville, RI; PW Engrg, Gulfport MS
NCBU 411 OIC, Norfolk VA

NCR 20, Commander
NMCB 133 (ENS T.W. Nielsen); 5, Operations Dept.; Forty, CO; One, LT F.P. Digeorge; THREE, Operations Off.
NRL Code 8441 (R.A. Skop), Washington DC
NROTCU Univ Colorado (LT D R Burns), Boulder CO
NSC E. Wynne, Norfolk VA
NUSC Code EA123 (R.S. Munn), New London CT; Code S332, B-80 (J. Wilcox); Code TA131 (G. De la Cruz), New London CT
OCEANAV Mangmt Info Div., Arlington VA
OCEANSYSLANT LT A.R. Giancola, Norfolk VA
ONR CDR Harlett, Boston MA; Code 484, Arlington VA; Dr. A. Laufer, Pasadena CA
PMTC Pat. Counsel, Point Mugu CA
PWC ACE Office (LTJG St. Germain); Code 116 (ENS A. Eckhart) Great Lakes, IL; Code 120C (A. Adams) San Diego, CA; Code 200, Great Lakes IL; Code 200, Oakland CA; Code 220 Oakland, CA; Code 30C (Boettcher) San Diego, CA; ENS J.A. Squatrito, San Francisco Bay, Oakland CA; Library, Subic Bay, R.P.; OIC CBU-405, San Diego CA; XO Oakland, CA
SPCC PWO (Code 120 & 122B) Mechanicsburg PA
US NAVAL FORCES Korea (ENJ-P&O)
USCG (G-ECV/61) (Burkhart) Washington, DC; MMT-4, Washington DC
USCG ACADEMY LT N. Stramandi, New London CT
USCG R&D CENTER CO Groton, CT; D. Motherway, Groton CT
USNA Ch. Mech. Engr. Dept Annapolis MD; PWD Engr. Div. (C. Bradford) Annapolis MD; Sys. Engr Dept (Dr. Monney), Annapolis MD
AMERICAN UNIVERSITY Washington DC (M. Norton)
CALIF. MARITIME ACADEMY Vallejo, CA (Library)
CALIFORNIA INSTITUTE OF TECHNOLOGY Pasadena CA (Keck Ref. Rm)
CALIFORNIA STATE UNIVERSITY LONG BEACH, CA (CHELAPATI); LONG BEACH, CA (YEN)
CITY OF CERRITOS Cerritos CA (J. Adams)
COLORADO STATE UNIV., FOOTHILL CAMPUS Engr Sci. Branch, Lib., Fort Collins CO
CORNELL UNIVERSITY Ithaca NY (Serials Dept, Engr Lib.)
DAMES & MOORE LIBRARY LOS ANGELES, CA
DUKE UNIV MEDICAL CENTER DURHAM, NC (VESIC)
FLORIDA ATLANTIC UNIVERSITY BOCA RATON, FL (MC *ALLISTER*); *Boca Raton FL* (Ocean Engr Dept., C. Lin)
FLORIDA ATLANTIC UNIVERSITY Boca Raton FL (W. Tessin)
FLORIDA TECHNOLOGICAL UNIVERSITY ORLANDO, FL (HARTMAN)
GEORGIA INSTITUTE OF TECHNOLOGY Atlanta GA (B. Mazanti)
INSTITUTE OF MARINE SCIENCES Morehead City NC (Director)
IOWA STATE UNIVERSITY Ames IA (CE Dept, Handy)
VIRGINIA INST. OF MARINE SCI. Gloucester Point VA (Library)
LEHIGH UNIVERSITY BETHLEHEM, PA (MARINE GEOTECHNICAL LAB., RICHARDS); Bethlehem PA (Fritz Engr. Lab No. 13, Beedle); Bethlehem PA (Linderman Lib. No. 30, Fleecksteiner)
LIBRARY OF CONGRESS WASHINGTON, DC (SCIENCES & TECH DIV)
MAINE MARITIME ACADEMY CASTINE, ME (LIBRARY)
MASSACHUSETTS INST. OF TECHNOLOGY Cambridge MA (Rm 10-500, Tech. Reports, Engr. Lib.); Cambridge MA (Rm 14 E210, Tech. Report Lib.); Cambridge MA (Whitman)
MICHIGAN TECHNOLOGICAL UNIVERSITY HOUGHTON, MI (HAAS)
MIT Cambridge, MA (Harleman)
NATL ACADEMY OF ENG. ALEXANDRIA, VA (SEARLE, JR.)
NY CITY COMMUNITY COLLEGE BROOKLYN, NY (LIBRARY)
OHIO STATE UNIVERSITY COLUMBUS, OH (INST. OF POLAR STUDIES)
OKLAHOMA STATE UNIV (Aziz Sharar), Stillwater, OK
OREGON STATE UNIVERSITY CORVALLIS, OR (CE DEPT, BELL); Corvalis OR (School of Oceanography); LT R.B. Steimer, NROTC Unit, Corvallis OR
PENNSYLVANIA STATE UNIVERSITY STATE COLLEGE, PA (SNYDER); UNIVERSITY PARK, PA (GOTOLSKI)
PURDUE UNIVERSITY LAFAYETTE, IN (ALTSCHAEFFL); Lafayette IN (Leonards); Lafayette, IN (CE LIB)
SAN DIEGO STATE UNIV. Dr. Krishnamoorthy, San Diego CA
SCRIPPS INSTITUTE OF OCEANOGRAPHY LA JOLLA, CA (ADAMS)
STANFORD UNIVERSITY STANFORD, CA (DOUGLAS)

STATE UNIV. OF NEW YORK Buffalo, NY; FORT SCHUYLER, NY (LONGOBARDI)
TEXAS A&M UNIVERSITY COLLEGE STATION, TX (CE DEPT); College TX (CE Dept, Herbich)
BONNEVILLE POWER ADMIN Los Angeles CA (Hancock Lib. of Bio. & Ocean)
UNIVERSITY OF CALIFORNIA BERKELEY, CA (CE DEPT, GERWICK); BERKELEY, CA (CE DEPT, MITCHELL); BERKELEY, CA (OFF. BUS. AND FINANCE, SAUNDERS); Berkeley CA (Dept of Naval Arch.); Berkeley CA (E. Pearson); DAVIS, CA (CE DEPT, TAYLOR); LIVERMORE, CA (LAWRENCE LIVERMORE LAB, TOKARZ); La Jolla CA (Acq. Dept, Lib. C-075A); SAN DIEGO, CA, LA JOLLA, CA (SEROCKI)
UNIVERSITY OF DELAWARE LEWES, DE (DIR. OF MARINE OPERATIONS, INDERBITZEN); Newark, DE (Dept of Civil Engineering, Chesson)
UNIVERSITY OF HAWAII HONOLULU, HI (CE DEPT, GRACE); HONOLULU, HI (SCIENCE AND TECH. DIV.); Honolulu HI (Dr. Szilard)
UNIVERSITY OF ILLINOIS URBANA, IL (DAVISSON); URBANA, IL (LIBRARY); URBANA, IL (NEWARK); Urbana IL (CE Dept, W. Gamble)
UNIVERSITY OF MASSACHUSETTS (Heronemus), Amherst MA CE Dept
UNIVERSITY OF MICHIGAN Ann Arbor MI (Richart)
UNIVERSITY OF NEBRASKA-LINCOLN LINCOLN, NE (SPLETTSTOESSER)
UNIVERSITY OF NEW HAMPSHIRE DURHAM, NH (LAVOIE)
UNIVERSITY OF NEW MEXICO Albuquerque NM (Soil Mech. & Pav. Div., J. Nielsen)
UNIVERSITY OF RHODE ISLAND KINGSTON, RI (PAZIS)
UNIVERSITY OF TEXAS Inst. Marina Sci (Library), Port Aransas TX
UNIVERSITY OF TEXAS AT AUSTIN Austin TX (R. Olson)
UNIVERSITY OF WASHINGTON Seattle WA (M. Sherif); M.A. Sherif, Seattle WA; SEATTLE, WA (APPLIED PHYSICS LAB); SEATTLE, WA (MERCHANT); SEATTLE, WA (OCEAN ENG RSCH LAB, GRAY); SEATTLE, WA (PACIFIC MARINE ENVIRON. LAB., HALPERN); Seattle WA (E. Linger)
US DEPT OF COMMERCE NOAA, Marine & Earth Sciences Lib., Rockville MD; NOAA, Pacific Marine Center, Seattle WA
US GEOLOGICAL SURVEY Off. Marine Geology, Mailstop 915, Reston VA
VENTURA COUNTY ENVIRONMENTAL RESOURCE AGENCY VENTURA, CA (MELVIN)
ATLANTIC RICHFIELD CO. DALLAS, TX (SMITH)
AEROSPACE CORP. Acquisition Group, Los Angeles CA
ALFRED A. YEE & ASSOC. Honolulu HI
ARCAIR CO. D. Young, Lancaster OH
AUSTRALIA Dept. PW (A. Hicks), Melbourne
BECHTEL CORP. SAN FRANCISCO, CA (PHELPS)
BELGIUM NAECON, N.V., GEN.
BETHLEHEM STEEL CO. BETHLEHEM, PA (STEELE)
BROWN & ROOT Houston TX (D. Ward)
CANADA Can-Dive Services (English) North Vancouver; Lockheed Petrol. Srv. Ltd., New Westminster BC; Mem Univ Newfoundland (Chari), St Johns; Surveyor, Nenninger & Chenevert Inc., Montreal; Univ. British Columbia (Finn), Vancouver, BC; Warnock Hersey Prof. Srv Ltd, La Sale, Quebec
CF BROWN CO Du Bouchet, Murray Hill, NJ
CHEVRON OIL FIELD RESEARCH CO. LA HABRA, CA (BROOKS)
CONCRETE TECHNOLOGY CORP. TACOMA, WA (ANDERSON)
DRAVO CORP Pittsburgh PA (Giannino)
NORWAY DET NORSKE VERITAS (Library), Oslo
EVALUATION ASSOC. INC KING OF PRUSSIA, PA (FEDELE)
FRANCE Dr. Dutertre, Boulogne; P. Jensen, Boulogne; Roger LaCroix, Paris
GEOTECHNICAL ENGINEERS INC. Winchester, MA (Paulding)
GLIDDEN CO. STRONGSVILLE, OH (RSCH LIB)
GLOBAL MARINE DEVELOPMENT NEWPORT BEACH, CA (HOLLETT)
GOULD INC. Shady Side MD (Ches. Inst. Div., W. Paul)
HALEY & ALDRICH, INC. Cambridge MA (Aldrich, Jr.)
HONEYWELL, INC. Minneapolis MN (Residential Engr Lib.)
ITALY M. Caironi, Milan; Sergio Tattoni Milano
LAMONT-DOHERTY GEOLOGICAL OBSERV. Palisades NY (McCoy); Palisades NY (Selwyn)
LOCKHEED MISSILES & SPACE CO. INC. SUNNYVALE, CA (PHILLIPS); Sunnyvale CA (Rynewicz)
LOCKHEED OCEAN LABORATORY San Diego CA (F. Simpson)
MARATHON OIL CO Houston TX (C. Seay)
MARINE CONCRETE STRUCTURES INC. MEFAIRIE, LA (INGRAHAM)

MC CLELLAND ENGINEERS INC Houston TX (B. McClelland)
MOBILE PIPE LINE CO. DALLAS, TX MGR OF ENGR (NOACK)
MUESER, RUTLEDGE, WENTWORTH AND JOHNSTON NEW YORK (RICHARDS)
NEW ZEALAND New Zealand Concrete Research Assoc. (Librarian), Porirua
NEWPORT NEWS SHIPBLDG & DRYDOCK CO. Newport News VA (Tech. Lib.)
NORWAY A. Torum, Trondheim; DET NORSKE VERITAS (Roren) Oslo; J. Creed, Ski; Norwegian Tech Univ (Brandtzaeg), Trondheim
OCEAN DATA SYSTEMS, INC. SAN DIEGO, CA (SNODGRASS)
OCEAN ENGINEERS SAUSALITO, CA (RYNECKI)
OCEAN RESOURCE ENG. INC. HOUSTON, TX (ANDERSON)
OFFSHORE DEVELOPMENT ENG. INC. BERKELEY, CA
PACIFIC MARINE TECHNOLOGY LONG BEACH, CA (WAGNER)
PORTLAND CEMENT ASSOC. SKOKIE, IL (CORELY); Skokie IL (Rsch & Dev Lab, Lib.)
PRESCON CORP TOWSON, MD (KELLER)
PUERTO RICO Puerto Rico (Rsch Lib.), Mayaquez P R
RAND CORP. Santa Monica CA (A. Laupa)
SANDIA LABORATORIES Library Div., Livermore CA
SCHUPACK ASSOC SO. NORWALK, CT (SCHUPACK)
SEATECH CORP. MIAMI, FL (PERONI)
SHELL DEVELOPMENT CO. Houston TX (E. Doyle)
SHELL OIL CO. HOUSTON, TX (MARSHALL); Houston TX (R. de Castongrene)
SWEDEN GeoTech Inst; VBB (Library), Stockholm
TIDEWATER CONSTR. CO Norfolk VA (Fowler)
TRW SYSTEMS REDONDO BEACH, CA (DAI)
UNITED KINGDOM Cement & Concrete Assoc. (R. Rowe), Wexham Springs, Slough B; D. New, G. Maunsell & Partners, London; Shaw & Hatton (F. Hansen), London; Taylor, Woodrow Constr (014P), Southall, Middlesex; Taylor, Woodrow Constr (Stubbs), Southall, Middlesex; Univ Bristol (Larnach), Bristol, England; University (Hanna), Sheffield, England
USGS MENLO PARK, CA (YOUD)
WESTINGHOUSE ELECTRIC CORP. Annapolis MD (Oceanic Div Lib, Bryan)
WISS, JANNEY, ELSTNER, & ASSOC Northbrook, IL (J. Hanson)
WM CLAPP LABS - BATTELLE DUXBURY, MA (LIBRARY); Duxbury, MA (Richards)
WOODWARD-CLYDE CONSULTANTS Oakland CA (A. Harrigan); PLYMOUTH MEETING PA (CROSS, III)
AL SMOOTS Los Angeles, CA
BULLOCK La Cañada
F. HENZE Boulder CO
CAPT MURPHY SAN BRUNO, CA
R.Q. PALMER Kaneohe HI
T.W. MERMEL Washington DC